



**NTNU – Trondheim**  
Norwegian University of  
Science and Technology

# Initial settlements of rock fills on soft clay

**Truls Martens Pedersen**

Civil and Environmental Engineering

Submission date: June 2012

Supervisor: Steinar Nordal, BAT

Co-supervisor: Gudmund Eiksund, BAT

Norwegian University of Science and Technology  
Department of Civil and Transport Engineering





Oppgavens tittel:	Dat0: 07/06-2012		
INITIAL SETTLEMENTS OF ROCK FILLS ON SOFT CLAY INTIALSETNINGER AV STEINFYLLINGER PÅ BLØT LEIRE	Antall sider (inkl. bilag): 80		
	Masteroppgave	X	Prosjektoppgave
Navn:	Truls Martens Pedersen		
Faglærer/veileder:	Gudmund Eiksund		
Eventuelle eksterne faglige kontakter/veiledere:			

<p>Ekstrakt:</p> <p>Rock fills that hit the seabed will remold the underlying material. If this material is a clay with sufficiently low shear strength, it will adopt rheological properties, causing flow through the rock fill, and contributing to the initial settlements of the rock fill in addition to conventional consolidation theory.</p> <p>The settlements of the rocks depend upon the height of the rock fill and how the rocks have been laid out. This is due to the viscosity of the clay, and the fact that clay is thixotropic. Thixotropy causes the viscosity to increase with decreased shear rate. The settlements finally come to a stop due to frictional forces from the surface area of the rocks.</p> <p>Clay is a non-newtonian Bingham fluid and will have a laminar flow through the rock fill. The Kozeny-Carman model is the most appropriate model for determining the permeability with laminar fluid flow through porous media.</p> <p>A clay with water content 52\% and shear strength 0,35kPa had a viscosity in a viscometer of <math>\eta = 7,8\text{Pas}</math>. Comparing theoretical and experimental results for immediate and layered loading of the rock fill showed clay viscosities of 7Pas and 40Pas respectively.</p>
--

#### Stikkord

1. Viscosity
2. rheology
3. soft clay
4. Kozeny-Carman
5. rock fill



## **preface**

This technical report has been written as part of the Master in Geotechnics program at NTNU, Trondheim, and was written over a course of 20 weeks from January to June. The report contains a literary review and description of experiments and simulations with regards to initial settlements of offshore rock fills on soft clay, and is meant for readers with basic knowledge in geotechnics and rheology.

The idea for the thesis was developed by my advisor, Professor Gudmund Eiksund, as a further study on the field of offshore rock fills on soft clay, which are mainly used for pipelines.

The thesis marks the final chapter of the education at NTNU, and is the end of a 5 year study program. It was developed for the most part by gathering information, performing experiments, and through discussions with my advisor. The last months have been filled with both excitement and frustration, but they have been very educational.

I would first and foremost like to thank my advisor, Professor Gudmund Eiksund, for all the help and time he put into this project. The door was always open and for that I am very grateful. This report would have been very different had it not been for him. I would also like to thank the staff at the geotechnical department at NTNU for their help with conducting experiments and computer programming. Lastly I would like to thank the geotechnical class of 2012 for always keeping the spirit up, even on late nights and stressful days.

## Abstract

Rock fills that hit the seabed will remold the underlying material. If this material is a clay with sufficiently low shear strength, it will adopt rheological properties, causing flow through the rock fill, and contributing to the initial settlements of the rock fill in addition to conventional consolidation theory.

The settlements of the rocks depend upon the height of the rock fill and how the rocks have been laid out. This is due to the viscosity of the clay, and the fact that clay is thixotropic. Thixotropy causes the viscosity to increase with decreased shear rate. The settlements finally come to a stop due to frictional forces from the surface area of the rocks.

Clay is a non-newtonian Bingham fluid and will have a laminar flow through the rock fill. The Kozeny-Carman model is the most appropriate model for determining the permeability with laminar fluid flow through porous media.

A clay with water content 52% and shear strength 0,35kPa had a viscosity in a viscometer of  $\eta = 7,8\text{Pas}$ . Comparing theoretical and experimental results for immediate and layered loading of the rock fill showed clay viscosities of 7Pas and 40Pas respectively.

## Sammendrag

Steinfyllinger som treffer sjøbunnen vil omrøre det underliggende materialet. Hvis dette materialet er en leire med tilstrekkelig lav skjærstyrke, vil den utvikle reologiske egenskaper, som skaper strømming gjennom steinfyllingen og bidrar til de initielle setningene av fyllingen i tillegg til konsolideringen.

Setningene av steinene er avhengig høyden på steinfyllingen og av hvordan steinene er lagt ut. Dette er på grunn av viskositeten til leiren, samt at leire er tiksotropisk. Tiksotropi fører til at viskositeten øker med minkende skjærhastighet. Setningene stanser til slutt på grunn av friksjonskrefter fra overflatearealet til fyllmassene.

Leire er en non-newtonian Bingham væske og har en laminær strømming gjennom en fylling. Kozeny-Carman modellen er den mest passende for å finne permeabilitet med laminær strømming gjennom porøst medium.

En leire med vanninnhold på 52% og skjærstyrke 0,35kPa hadde en viskositet på  $\eta = 7,8\text{Pas}$ . En sammenligning av teoretiske- og forsøksresultater for umiddelbar og lagvis senking av steinfyllingen ga forholdsvis 7Pas og 40Pas i viskositet for leiren.

# Contents

<b>1</b>	<b>Introduction</b>	<b>7</b>
<b>2</b>	<b>Theory</b>	<b>11</b>
2.1	Conventional theory of consolidation . . . . .	11
2.2	Settlements of rock fills . . . . .	13
<b>3</b>	<b>Rheology</b>	<b>15</b>
3.1	Shear rate . . . . .	15
3.2	Viscosity . . . . .	16
3.2.1	Dynamic and kinematic viscosity . . . . .	16
3.2.2	Complex viscosity . . . . .	17
3.2.3	Flow- and viscosity curves . . . . .	17
3.2.4	The yield point . . . . .	18
3.3	Non-newtonian fluids . . . . .	19
3.3.1	Bingham fluids . . . . .	20
3.4	Thixotropy . . . . .	21
3.5	Porosity and void ratio . . . . .	22
3.6	Permeability . . . . .	24
3.6.1	Intrinsic permeability . . . . .	24
3.6.2	Tortuosity . . . . .	24
3.6.3	Surface area $S_0$ and shape factor $C_s$ . . . . .	25
3.6.4	Diameter . . . . .	26
3.6.5	Determining the permeability . . . . .	27
<b>4</b>	<b>Laboratory experiments</b>	<b>29</b>
4.1	Routine parameters . . . . .	30
4.1.1	Analyzing results . . . . .	31
4.1.2	Water content vs. shear strength . . . . .	32
4.2	Finding the thixotropy . . . . .	33
4.3	Description of the experiment . . . . .	33
4.4	Experiment using Laponite . . . . .	36

4.4.1	Results and discussion, Laponite . . . . .	37
4.5	Experiment using clay . . . . .	39
4.5.1	Experiment 1 . . . . .	39
4.5.2	Experiment 2 . . . . .	44
4.5.3	Experiment 3 . . . . .	48
4.6	Finding the viscosity . . . . .	52
4.6.1	Viscosity measurements using a ConTek viscometer . . . . .	53
<b>5</b>	<b>Theoretical simulation model</b>	<b>59</b>
5.1	Description . . . . .	59
5.2	Parameters, descriptions and empirical values . . . . .	59
5.3	Construction . . . . .	60
5.4	Comparing experiments and simulations . . . . .	62
<b>6</b>	<b>Conclusion</b>	<b>65</b>
<b>7</b>	<b>Recommended future work</b>	<b>67</b>
<b>A</b>	<b>Background and task description</b>	<b>69</b>
<b>B</b>	<b>CD</b>	<b>71</b>



# List of Figures

1.0.1 Example of rock fills for pipelines . . . . .	8
1.0.2 Fall pipe for rock fill . . . . .	8
2.1.1 Primary settlements . . . . .	12
2.1.2 Secondary settlements . . . . .	12
2.2.1 Material flow through porous rock fill . . . . .	14
3.1.1 A fluid element straining at rate $\delta\Theta/\delta t$ . . . . .	15
3.2.1 Flow and viscosity curves . . . . .	18
3.2.2 Flow (left) and viscosity (right) curves showing fluids with and without an apparent yield point . . . . .	19
3.3.1 Simple shear . . . . .	19
3.3.2 Bingham fluid . . . . .	21
3.4.1 Shear stress vs. shear rate for thixotropic and rheopectic materials . . . . .	22
3.5.1 Pore volume for different materials . . . . .	23
3.5.2 Effective and ineffective pores . . . . .	23
4.0.1 Leangbukta . . . . .	29
4.1.1 Grain size distribution . . . . .	30
4.1.2 water content vs. shear strength . . . . .	32
4.3.1 Empty cylinder with supports . . . . .	35
4.3.2 Devices used for measuring . . . . .	36
4.4.1 Experiment using Laponite . . . . .	37
4.4.2 Air bubbles in the Laponite . . . . .	38
4.5.1 Cylinder filled with clay and rocks, supported by the piston at the bottom . . . . .	40
4.5.2 Cylinder filled with clay and rocks, supported by the piston at the bottom . . . . .	41
4.5.3 Pressure with time . . . . .	42
4.5.4 Pressure vs. deformation . . . . .	43
4.5.5 New support for the cylinder . . . . .	45
4.5.6 Pressure with time 2 . . . . .	46
4.5.7 Pressure vs. deformation 2 . . . . .	47
4.5.8 Pressure with time 3 . . . . .	50

4.5.9 Pressure vs. deformation 3 . . . . .	50
4.6.1 The two-plate model and a visualization of the shear force and deformation .	52
4.6.2 The cone and plate oscillatory measuring system . . . . .	53
4.6.3 Viscometer . . . . .	54
4.6.4 Setup used in program to find viscosity . . . . .	55
4.6.5 Example of a graph produced by a viscometer . . . . .	55
4.6.6 Torque vs. rotations velocity with fitted line produced by viscometer . . . . .	57
5.3.1 Example of graph obtained from worksheet . . . . .	61
5.4.1 Comparison of settlements in simulation and experiment 2 . . . . .	62
5.4.2 Comparison of settlements in simulation and experiment 3 . . . . .	63

## List of Tables

4.1	Routine parameters . . . . .	30
4.2	Comparison with soils from Ormen Lange[7] . . . . .	31
4.3	Water content vs. shear strength . . . . .	32
4.4	Thixotropy . . . . .	33
4.5	Clay data for experiment 1 . . . . .	42
4.6	Clay data for experiment 2 . . . . .	46
4.7	Clay data for experiment 3 . . . . .	49
4.8	Values obtained from viscometer test . . . . .	56
4.9	default . . . . .	57



## Chapter 1

# Introduction

Rock fills are frequently used as foundations for seabed structures and pipelines in offshore construction. The rock fill consists of crushed rocks with grain size 5-15cm, and are usually installed using a fall pipe vessel. They can be constructed with a vertical tolerance of +/- 0,2 meters at more than 1000 meters water depth. A very important design criterion for structures placed on the seabed is the long term settlements of the rock fills. These settlements are assumed to follow conventional primary and secondary (creep) consolidation theory. However, on soft seabed ( $s_u < 2$  kPa) there have been frequent observations of settlements that are not following conventional consolidation theory. In some cases the observed settlements after a couple of months are the same for a rock fill with a height of 0,5m as for a rock fill with a height of 2m (about 0,3m settlement for both). If the settlement is only controlled by consolidation the settlement would be nearly proportional to the height of the rock fill.

There are several possible explanations to this phenomenon, with one theory being that the observed settlement is controlled by a liquid flow of soft clay through the voids of the rock fill. This process can be compared to normal fluid flow through a porous medium. However, here the flow will be governed by rheological parameters as well as geotechnical properties, e.g., the remolded shear strength, the viscosity, and the thixotropy of the clay material.

Without knowledge of the physical process controlling the initial settlement, the observed settlements can not be used to calibrate a theoretical calculation model for the long term settlement. A better understanding of the initial settlements is therefore important for a more accurate prediction of the long term settlement of offshore rock fills.

Offshore conditions are hard to replicate as an experiment in the lab because several assumptions will have to be made, which increases the margin for error. However, a visualization or simulation of the phenomenon will give answers in terms of the validity of the hypothesis, as well as a basis for constructing a calculation model that can combine parameters in order to predict the rock fill settlements.

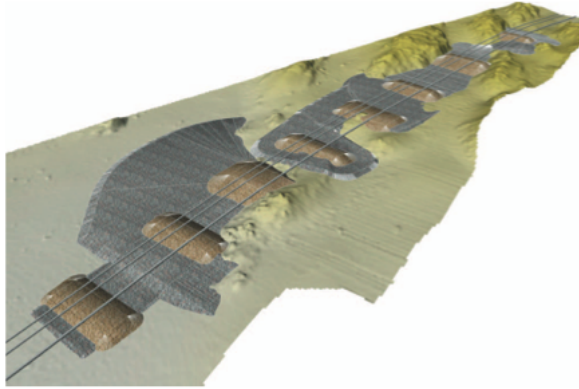


Figure 1.0.1: Example of rock fills for pipelines  
[10]

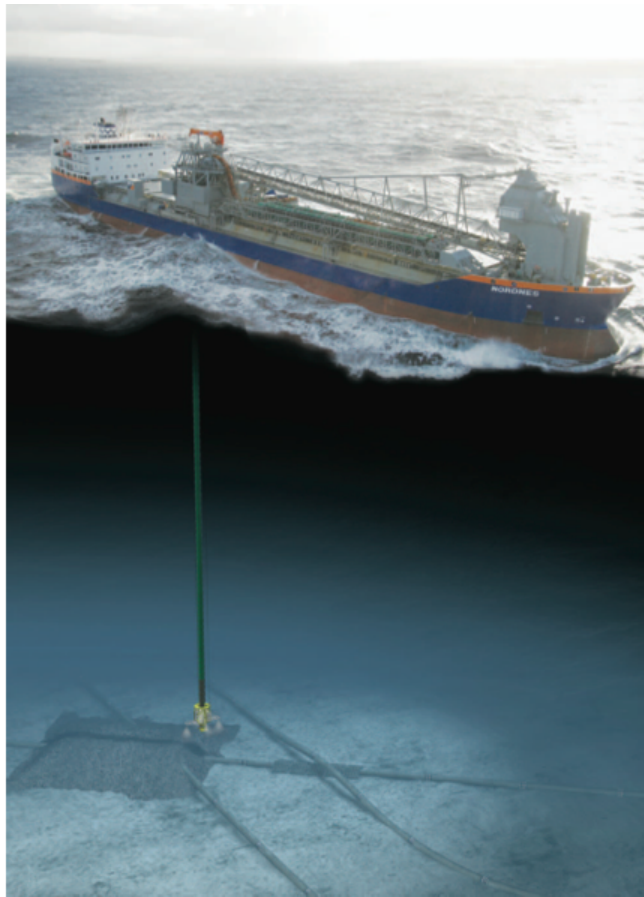


Figure 1.0.2: Fall pipe for rock fill  
[10]

## **Report outline**

The report consists of 7 chapters including the introduction, and in the end a CD with appendices:

- The second chapter gives a brief summary of conventional consolidation theory and total settlements of offshore rock fills.
- The next chapter is a literature review on rheological parameters, especially related to clay flow in a porous medium.
- Further on there is a chapter describing the experiments performed, and the results obtained from these experiments.
- Next comes a description of the construction and use of a theoretical simulation model.
- In chapter 6 the report has been summarized and conclusions are presented.
- Finally in chapter 7 a suggestion for recommended future work on this field is given.
- Appendices: The appendices consist of theoretical worksheet models for immediate loading and layered loading, the data from the viscometer tests, and a video of the experiment for immediate loading. All the appendices have been gathered on a CD as this will be more useful to the reader.





## Chapter 2

# Theory

### 2.1 Conventional theory of consolidation

The consolidation of a material is usually linked to the settlements of a structure. By determining the consolidation behavior of a material, one can predict the settlements that will occur within a certain time perspective. Although the settlements will decrease significantly with time, they never really come to a complete stop. The consolidation is usually described in three intervals, or by three contributions:

- *Immediate settlement,  $\delta_i$* : These settlements happen when the total load has been placed and time is set equal to zero. This is often at the end of the construction period. The immediate settlements occur due to a change in the shape while the volume is constant. The water flow is inconsequential in soils with low permeability, and there will be a build up of excess pore water pressure. For more pervious soils the water flows more rapidly and there will be a change in volume. In the case of pervious soils the flow of water is quick at constant volume. Elastic theory governs this phenomenon [11].
- *Primary settlements,  $\delta_p$* : These are the settlements that happen in the primary consolidation time  $t_p$ , which is described as the time until all the pore pressure has dissipated ( $\Delta u = 0$ ). These settlements are slow and the movement of water depends on the permeability of the soil. With time the water pressure dissipates and the flow of water stops. As this happens there will be an increase in effective stresses in the soil as can be seen in the graph below(2.1.1). This interval is defined from the time water starts to flow out of the voids until the time it ceases. This compression is also known as the consolidation settlement[11][22].

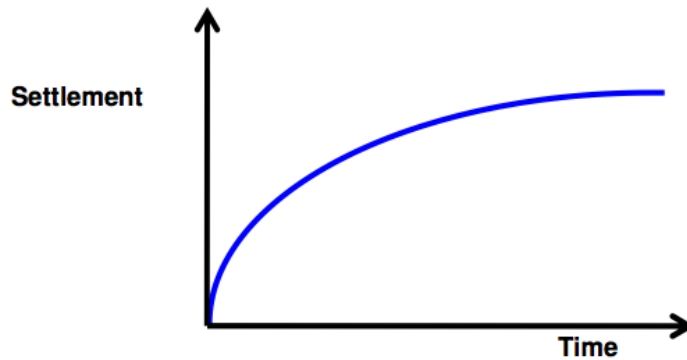


Figure 2.1.1: Primary settlements  
[11]

- *Secondary settlements,  $\delta_s$* : These settlements are time-dependent and will never fully stop. They are dominated by creep and occur due to gradual changes in the particle structure of the soil. The rate of the secondary consolidation is much slower than for the primary consolidation, and depending on the material, many years will go by before the structure is considered to be "fully" settled(2.1.2)[11][22].

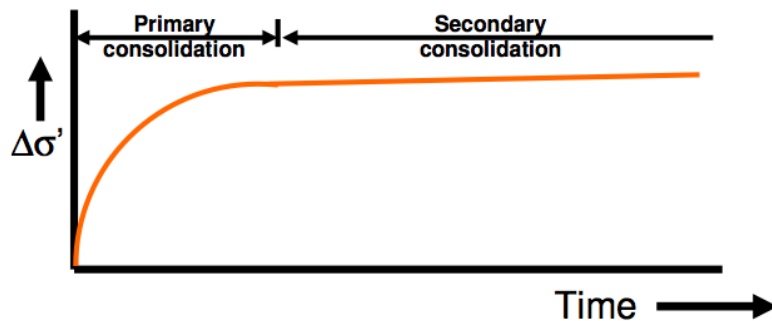


Figure 2.1.2: Secondary settlements  
[11]

It is difficult to determine the actual transition from one consolidation phase to another, as they usually overlap, e.g., creep in the material will normally have started before all the pore water has dissipated. This is especially true for clay materials [22]. In this report it is the deviation from the conventional consolidation theory for immediate settlements that is in question. Presumably the primary and secondary settlements follow the expected behavior, but they will both be affected by the fact that the immediate settlements here depend upon other parameters than usual.

## 2.2 Settlements of rock fills

Methods for measuring the immediate settlements of rock fills on offshore soft clay have been developed, and results show that the theoretical values are coherent with the measured values for actual projects. The standard deviation, however, is quite high in most of these cases, and a deeper understanding of how the settlements behave is therefore necessary. In theory, the initial settlements of rock fills consists of four parts[10]:

- *surface erosion*
- *penetration of individual rock parcels*
- *material flow into the rock skeleton*
- *immediate deformation*

In this report material flow into the rock skeleton will be the main focus. However, a brief explanation of each contribution to the settlements is given below:

### **Surface erosion**

When the rocks are installed on the seabed, a flow of masses is created inside the fall pipe system. The velocity of this mass is about 4 m/s. When this mass reach the end of the pipe, and is projected into the water, a jet of water is formed. This jet pushes or flushes away the weak top layer of clay on the seabed. This is called surface erosion. The thickness of the eroded layer depends on the conditions on that location, but realistic assumptions would be 0,1-0,15 meter. This is why information retrieved from the top 0,5 meters of the soil on the seabed are not very reliable[10].

### **Penetration of individual rock particles.**

As the rock fill hits the seabed, individual rocks of different sizes will penetrate into the soft clay. The depth of the penetration depends in the size of the particle, the velocity at impact, and the soil conditions. There are several formulas developed for determining the penetration of rocks into a subsoil[10].

### **Material flow into the rock skeleton**

Due to the impact of the rock fill on the seabed, the soft clay will be remolded. This weakens the shear strength, and makes the clay behave similarly to a liquid. For small loads, the surface is stable, but as soon as more pressure is applied the contact stress between rocks and clay will increase. This leads to farther penetration of the rock fill into the clay, until a new equilibrium is reached (see figure 2.2.1)[10].

### immediate deformation

This contribution has been explained in section 2.1 as part of the conventional consolidation theory of clay. The immediate deformations happen when the entire rock fill is in place, and are changes in shape without volume change.

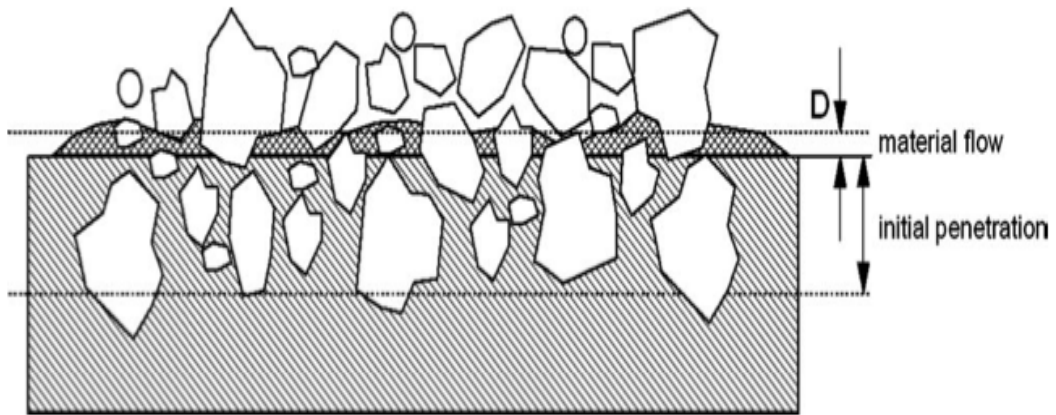


Figure 2.2.1: Material flow through porous rock fill  
[10]

## Chapter 3

# Rheology

### 3.1 Shear rate

The shear rate can be described as the gradient of velocity of fluid flow, or *"the rate of change of velocity at which one layer of fluid passes over an adjacent layer"*[24]. In order to find the shear rate of a liquid, it is placed between two plates, and the top plate is pulled with a known force. The velocity of the movement of the top plate is then measured and the shear rate can be found from the formula:

$$\dot{\gamma} = \frac{v}{h} \quad (3.1.1)$$

where  $v$  is the velocity in meters per second and  $h$  is the distance between the two plates in meters. A model showing the parameters of the model can be seen in figure 3.1.1. The unit for the shear rate is given as a "reciprocal second" or [1/s][18].

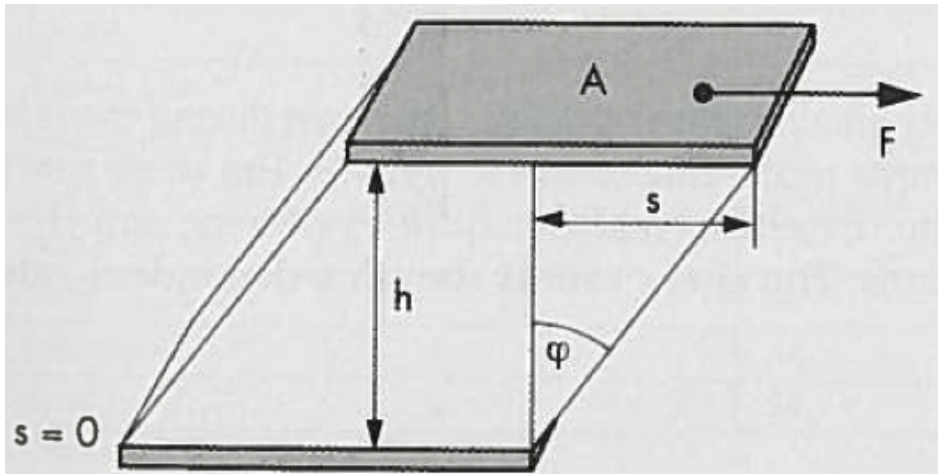


Figure 3.1.1: A fluid element straining at rate  $\delta\Theta/\delta t$

## 3.2 Viscosity

Viscosity is a quantitative measurement of a fluid's resistance to flow due to frictional forces between the molecules. This is expressed as the strain rate of the fluid for a given applied shear stress. Fluid in this context means both liquids and gases. Air has a very low viscosity, which is why we can easily move through it. Water has a higher viscosity, almost 50 times more than air, and is therefore harder to move through. Yet a higher resistance can be found in, e.g., cake dough or motor oil[27].

One does not normally consider a solid material like clay to have a viscosity, but in the case of clays with very low shear strength or high water contents, the clay will act comparatively to a fluid when remolded. Temperature greatly affects the viscosity, increasing with T for gases, and decreases in liquids. Pressure will also have an effect on the viscosity, although it only gives a small increase with increasing pressure. Hence the pressure variation is usually neglected in most engineering practices[27].

The viscosity coefficient will in this report be expressed as the greek letter  $\eta$ , and is related to the shear strength and the shear rate in ideal-viscous or Newtonian fluids at constant temperature by the formula[18]:

$$\tau = \eta \frac{\delta \Theta}{\delta t} = \eta \frac{\delta u}{\delta y} = \eta \dot{\gamma} \quad (3.2.1)$$

The unit used to express viscosity is [Pa\*s] (here: [Pas]) or Pascalseconds, giving the following relationship:

$$1Pas = 1N * s/m^2 = 1kg/s * m \quad (3.2.2)$$

When dealing with low-viscosity fluids, the most commonly used unit is millipascalseconds;  $1 \text{ mPas} = 10^{-3} \text{ Pas}$  In older articles about viscosity the unit "poise" [P] is used to express viscosity, sometimes confusing the reader. This gives the relationship:  $1 \text{ P} = 100 \text{ cP} = 0,1 \text{ Pas} = 100 \text{ mPas}$ . Hence:  $1 \text{ cP} = 1 \text{ mPas}$ [18].

In many papers the letter  $\mu$  is used to express the viscosity, which can sometimes be confusing.

### 3.2.1 Dynamic and kinematic viscosity

$\eta$  is sometimes used to describe the "dynamic viscosity" of a fluid. However, the term dynamic viscosity is also used when referring to the complex viscosity, or the real part of the complex viscosity, which can create some confusion. To avoid this  $\eta$  (without the star) will be referred to as the dynamic viscosity or simply the viscosity, and to  $\eta^*$  as the complex viscosity with its real and imaginary components.

The potential or kinematic viscosity is used when relating the viscosity to the permeability

of two different materials, and is defined as:

$$\nu = \frac{\eta}{\rho} \quad (3.2.3)$$

The unit for kinematic viscosity is  $[mm^2/s]$ , but Stokes [St] was previously used, giving the relationship  $1 mm^2/s = 1 \text{ cSt}$ .[\[18\]](#)

### 3.2.2 Complex viscosity

Following Hooke's law and the relation between the shear stress and shear strain we get:

$$\tau(t) = G^* * \gamma(t) \quad (3.2.4)$$

Where  $G^*$  is the complex shear modulus. In oscillatory tests  $G^*$  represents the sample's resistance to deformation. Parameters that result from a periodical or sinusoidal load are presented on the complex form, i.e., adding a star to the notation. This is in order to differentiate it from the "regular" notation, which is not measured with an oscillatory test[\[18\]](#). If we assume a viscoelastic behavior in the material,  $G^*$  has to have a viscous and an elastic part. We get:

$$G^* = \sqrt{(G')^2 + (G'')^2} \quad (3.2.5)$$

In this equation  $G''$  represent the irreversible viscous deformation of the material, and  $G'$  is the elastic behavior. If we then apply Newton's law for stress and strain relation for a fluid[\[14\]](#):

$$\sigma = \eta * \epsilon \quad (3.2.6)$$

we can determine the complex viscosity  $\eta^*$  of a fluid[\[14\]](#).

$$\eta^* = \frac{\tau(t)}{\dot{\gamma}(t)} \quad (3.2.7)$$

As  $\eta^*$  is also a complex value, we can split it into a real and an imaginary part,  $\eta'$  and  $\eta''$  respectively. The real part represents the viscous behavior and the imaginary part represents the elastic behavior defined by the relationship[\[18\]](#):

$$|\eta^*| = \sqrt{(\eta')^2 + (\eta'')^2} \quad (3.2.8)$$

### 3.2.3 Flow- and viscosity curves

When using a rheometer to measure the viscosity of a fluid, the results are presented in flow- and viscosity curves. These curves represent the behavior of the flow. The flow curve shows the relationship between the shear stress,  $\tau$ , on the y-axis, and the shear rate,  $\dot{\gamma}$ , on the x-axis. The viscosity of newtonian liquids[\(3.3\)](#) can also be found by using flow cups or viscometers, although these methods do not describe the complex behavior of a non-newtonian fluid, and

are therefore not ideal[18].

From the flow curve one can find the viscosity curve, with  $\dot{\gamma}$  on the x-axis and  $\eta$  on the y-axis. Figure 3.2.1 shows a comparison of the flow (3.2.1a) and viscosity (3.2.1b) curves of fluids with different properties. Each line in the figure represents one of the characteristic explained below[18]:

- 1: idealviscous (newtonian)
- 2: Shear-thinning
- 3: Shear-thickening

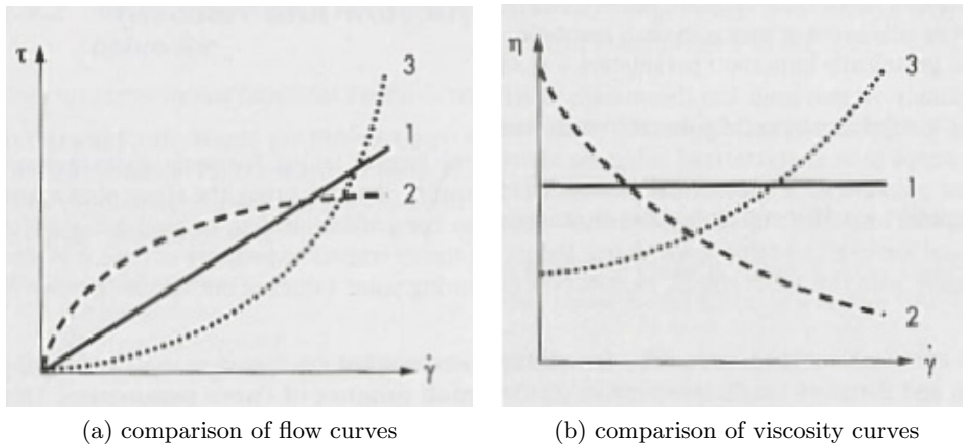


Figure 3.2.1: Flow and viscosity curves [18]

### 3.2.4 The yield point

Some fluids have a yield point  $\tau_0$ , and only begin to flow when the external acting force is larger than the internal structural forces in the liquid. These are commonly called non-newtonian fluids (3.3). Prior to reaching the yield point the material has an elastic behavior, i.e., only shows small deformations that disappear when the load is removed[18]. An example of a fluid that has such a yield point is mayonnaise, which only starts to flow when sufficient pressure is applied. Figure 3.2.2 shows the flow (left) and viscosity (right) curves of fluids with and without an apparent yield flow[18]:

- 4: No yield point
- 5: Apparent yield point



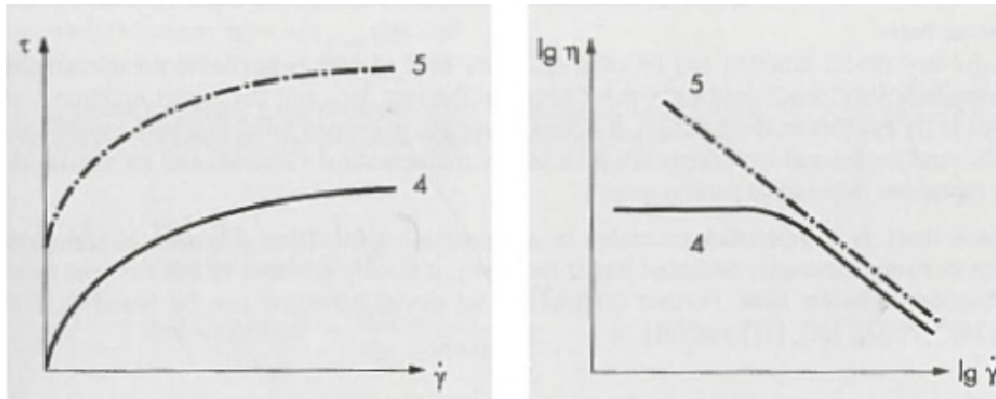


Figure 3.2.2: Flow (left) and viscosity (right) curves showing fluids with and without an apparent yield point

[18]

### 3.3 Non-newtonian fluids

In order to explain the concept of non-newtonian fluids, a definition of a newtonian fluid will be given: most low molecular weight substances show newtonian flow characteristics. That means that in simple shear at constant temperature and pressure, the shear stress,  $\sigma$ , is proportional to the shear rate,  $\dot{\gamma}$ , where the dynamic viscosity,  $\eta$ , is constant. In simple shear (figure 3.3.1), the response of a newtonian fluid is recognized by a linear relationship between the applied shear stress and the shear rate[8]:

$$\sigma_{yx} = \frac{F}{A} = \eta \dot{\gamma} \quad (3.3.1)$$

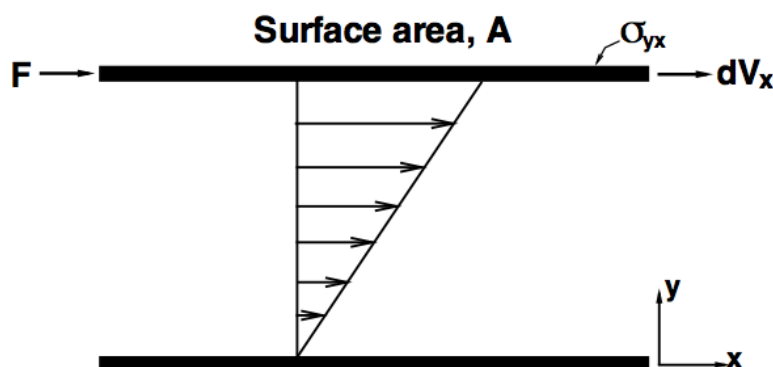


Figure 3.3.1: Simple shear

During the last decades, there has been a broader understanding of viscous fluids and of the fact that many substances such as foams, emulsions, dispersions, suspensions, and slurries do not follow the characteristics of a newtonian fluid, i.e., a linear relationship between  $\sigma$  and  $\dot{\gamma}$  in simple shear. These fluids have therefore been commonly known as non-newtonian, non-linear, or complex. The most obvious difference between a non-newtonian and a newtonian fluid is when the simple shear relationship  $\sigma - \dot{\gamma}$  does not pass through origin and/or does not follow a linear path. As a consequence, the viscosity, which was previously defined as  $\sigma/\dot{\gamma}$ , will not be constant, i.e., is a function of  $\sigma$  or  $\dot{\gamma}$ . Once established as a non-newtonian fluid, the fluid has to be further divided within three categories. These categories are not scientifically established, but work as a pinpoint for the difference between non-newtonian fluids[8].

1. Systems where the value of  $\dot{\gamma}$  at a point in the fluid is determined only by the current value of  $\sigma$  at that point. Known as as inelastic, time-independent, or generalized newtonian fluids.
2. Systems where the duration of shearing and the kinematic history influence the relation between  $\sigma$  and  $\dot{\gamma}$ . These fluids are commonly known as time-dependent.
3. Fluids that show partial elastic recovery, recoil, or creep. They usually show a mixture if viscous and elastic solid-like behavior. These fluids are called visco-elastic or elastic-viscous.

This way of classifying is rather random, but it is a good way of distinguishing between the different types, although most fluids show characteristics a combination of two or even all three of these categories, e.g., a china clay can have both time-independent (shear-thinning) and time-dependent (thixotropic) features at certain concentrations and/or the right shear rate[8]. Here only fluids with shear-thinning properties will be considered, as clay materials fall into this category.

### 3.3.1 Bingham fluids

A Bingham fluid is a type of non-newtonian fluid that has an apparent yield point. In simple shear of a Bingham fluid, the fluid will show no movement if the shear stress applied does not surpass a certain threshold or yield point,  $\tau_0$  (3.2.4). Before this threshold has been crossed, the Bingham fluid behaves like an incompressible newtonian fluid. Mathematically the phenomenon can be explained like this[2]:

$$\tau < \tau_0 \Rightarrow \dot{\gamma} = 0 \tag{3.3.2}$$

$$\tau > \tau_0 \Rightarrow \dot{\gamma} = \frac{1}{\eta}(\tau - \tau_0) \tag{3.3.3}$$

A Bingham fluid is expressed graphically in figure 3.3.2:

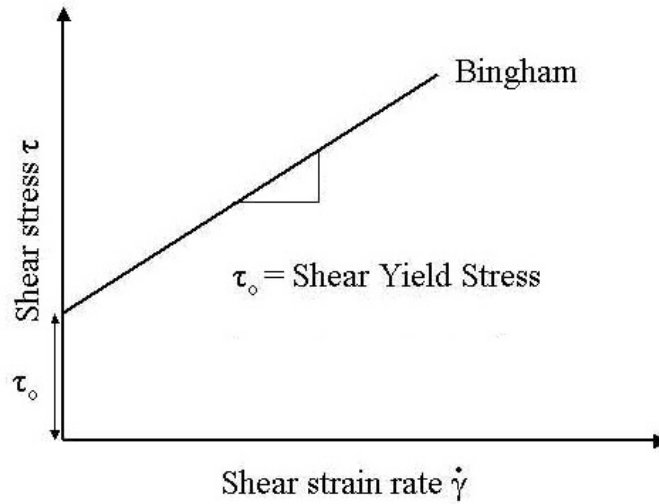


Figure 3.3.2: Bingham fluid  
[1]

Bingham fluids show a linear plastic behavior after the yield point has been passed. The inclination of the graph is the viscosity of the material. This type of fluid is normal for paint, toothpaste, ketchup, and granular suspensions, such as some types of clay[2].

### 3.4 Thixotropy

Thixotropy can be defined as *"a process of softening caused by remolding, followed by a time dependent return to the original harder state at a constant water pressure and constant porosity"*[3]. Thixotropy relates to viscosity through the fact that a thixotropic fluid shows a higher viscosity when stirred slowly than it does when stirred more rapidly. Hence the energy needed to move the fluid is not directly equal to the speed at which it is moved.

A material is regarded as thixotropic if when sheared at a constant rate, the viscosity  $\eta = \sigma/\dot{\gamma}$  decreases with the duration of shearing. If the flow curve of a thixotropic fluid is measured in a single experiment where the shear rate is increased at a constant rate to some maximum value and then decreased at the same rate, a hysteresis loop will form, as can be seen in figure 3.4.1 [8]. The area and the height of the loop will depend on the natural properties of the material and on the experimental conditions, e.g., the rate of shearing or maximum value of shear rate. The larger the enclosed area, the more significant is the time-dependent behavior of the material. This means that for a purely viscous fluid the area would be zero. Fluids that show a negative thixotropic behavior are called rheopectic materials. In these fluids the viscosity increases with time of shearing. Here the hysteresis loop will be inverted[8].

For this report the clay material in question will be assumed to have both Bingham fluid and a thixotropic or time-dependent characteristics.

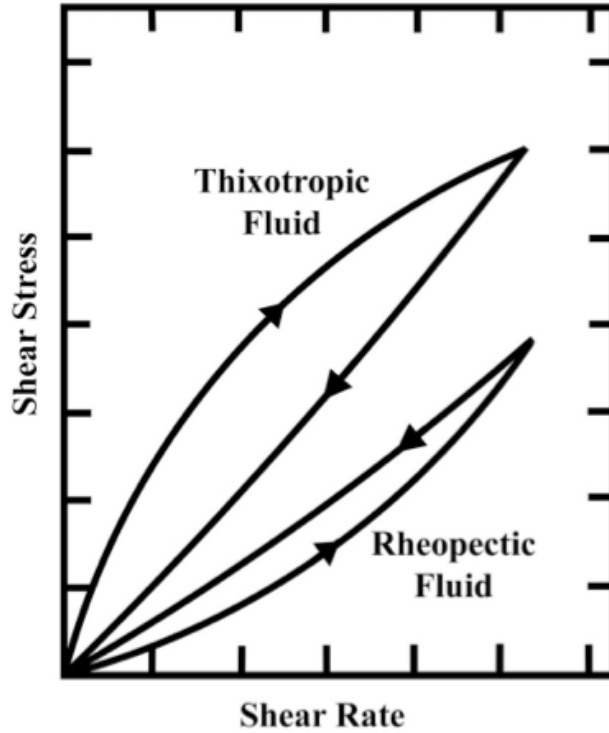


Figure 3.4.1: Shear stress vs. shear rate for thixotropic and rheopectic materials

### 3.5 Porosity and void ratio

The porosity,  $n$ , and the void ratio,  $e$ , are both measures of the compaction of the mass of a material. They give an indication of the magnitude of the pore volume. The porosity is the relationship between the volume of the pores,  $V_p$ , and the total volume of the sample,  $V$ :

$$n = \frac{V_p}{V} \quad (3.5.1)$$

The porosity of sand can vary from 0,25 to 0,60, and for clay the it is usually somewhere between 0,30 and 0,80. The porosity of rock fills that have been dropped from a height is usually assumed to be 0,4.

The void ratio is the ratio of the pore volume,  $V_p$ , to the volume of solid material,  $V_s$ :

$$e = \frac{V_p}{V_s} \quad (3.5.2)$$

$n$  and  $e$  are usually given in percent and they are related by this equation[21]:

$$n = \frac{V_p}{V} = \frac{V_p}{V_s + V_p} = \frac{V_p/V_s}{1 + V_p/V_s} = \frac{e}{1 + e} \quad (3.5.3)$$

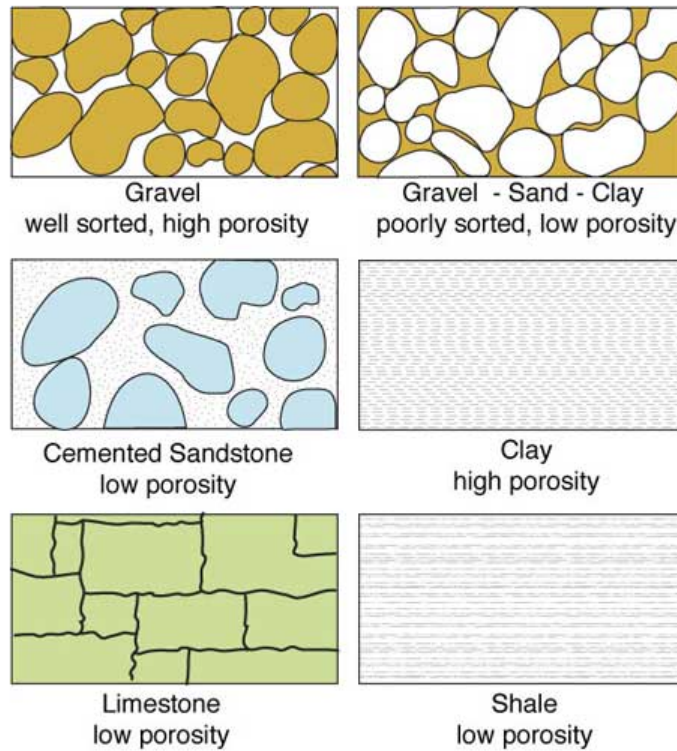


Figure 3.5.1: Pore volume for different materials [26]

The porosity can be divided into effective and ineffective porosity. Effective pores are then separated into Cul-de-sac or dead-end pores, and catenary pores. Dead-end pores only have one "exit" while catenary pores have two or more. Ineffective pores have no "exits" and are simply a hollow space in the material. This can be seen below in figure 3.5.2[16].

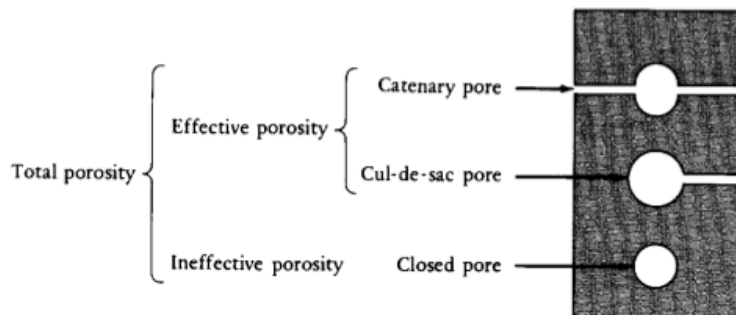


Figure 3.5.2: Effective and ineffective pores [16]

### 3.6 Permeability

Permeability is defined as: *"The ability of a substance to allow another substance to pass through it, especially the ability of a porous rock, sediment, or soil to transmit fluid through pores and cracks"*[15].

Best known for his studies on permeability is Henry Darcy, and his work forms the basis for most of the formulas used today. Darcy's law states that: *"the volumetric flow of rate  $Q$  of a liquid through a specimen of porous material is proportional to the difference in pressure,  $\Delta h$ , across the specimen, inversely proportional to the length,  $L$ , of the specimen, and proportional to the cross section area,  $A$ "*[19]. Together these form Darcy's law for flux:

$$Q = \frac{kA\Delta h}{L} \quad (3.6.1)$$

where  $k$  is the permeability. This equation transforms into the more common manner of expressing Darcy's formula; in terms of the velocity,  $v$ :

$$v = k \frac{\Delta h}{L} \quad (3.6.2)$$

The permeability is usually not spatially uniform or isotropic, but is often displayed that way in theory for the sake of simplicity. In most cases it varies with direction and depends on the stress conditions and stress history.

#### 3.6.1 Intrinsic permeability

The permeability described above in 3.6 depends on both the porous material and on the fluid that passes through it. In laminar flows the permeability,  $k$ , varies inversely with the fluid's viscosity,  $\eta$ . It is therefore possible to define an intrinsic permeability,  $k'$ , which is a parameter that is independent of the fluid used to measure it, and that has the dimension  $m^2$ . These two material permeability properties essentially describe the same phenomenon, but the fact that they are usually expressed by the same name while depending on different parameters can be confusing. Both definitions are widely used, although  $k$  more than  $k'$ . Converting from one of the properties to the other is straightforward, and depends on the viscosity, and the density,  $\rho$ , of the fluid at a given temperature[19].

$$k' = \frac{k\eta}{\rho g} \quad (3.6.3)$$

#### 3.6.2 Tortuosity

The Blake-Kozeny model(3.6.5) is a way of determining the viscosity of a fluid in a porous medium in relation to the particles of the medium. Generally the model represents the network of pores in the porous medium as an accumulation or bundle of capillary tubes with a determined average radius,  $R$ , and an average length,  $L'$ . The effective radius is related to

the particle diameter,  $d$ , through the concept of hydraulic radius. The model also assumes that the particles in the porous medium resembles a bed of uniform spheres. Due to the fact that the length the fluid has to travel in the porous medium is longer than the system length,  $L$ , which represents straight capillary tubes, the model introduces the previously mentioned parameter,  $L'$ . This phenomenon is called tortuosity of the pore network.

$$\tau = \left(\frac{L'}{L}\right)^2 \quad (3.6.4)$$

where  $\tau$  is the tortuosity factor and has been empirically determined to be 25/12:

$$\tau = \left(\frac{L'}{L}\right)^2 = \frac{25}{12} \quad (3.6.5)$$

As mentioned above, this factor assumes circular channels in the pores, which is of course not the case in for instance a rock fill. Tests using rectangular tubes performed by Kozeny showed that a more appropriate factor for the tortuosity is 2,5. When performing the experiments to determine this constant Kozeny used tubes in straight lines though the pores, and when Carman used an actual porous medium for his experiments, results showed that the fluid actually moves at a 45 degree angle to the straight flow through the pores. This gives the length the liquid has to move[5]:

$$L' = \sqrt{2}L \Rightarrow \left(\frac{L'}{L}\right)^2 = 2 \quad (3.6.6)$$

Multiplying with the factor for rectangular tubes 2,5 gives a correction factor of 5. this factor has later been confirmed to be reasonable when dealing with with laminar flow in a porous medium[5], and this is therefore the factor that will be used here. This value can also be measured as a function of the porosity of the porous media.[17]

### 3.6.3 Surface area $S_0$ and shape factor $C_s$

The area of the particles in the porous media that a fluid covers can be very important when dealing with liquid flow. The surface has a tendency to act as a dragging force on the flow due to viscous shear or friction between the fluid and the particles. In order to determine the surface area of a medium one can multiply the area of one grain with the number of grains within a volumetric unit[5]:

$$S_0 = 4\pi r^2 * n = 4\pi r^2 * \frac{3}{4\pi r^3} = \frac{3}{r} \quad (3.6.7)$$

The derivation of this formula can be found in [5]. However, all parts of a porous medium is not made up of solids. The pores make up a large part of the volume, so the amount of

solids within a bulk volume is given by  $1 - n$ [5]:

$$S = \frac{3 * (1 - n)}{r} \quad (3.6.8)$$

These formulas for determining the surface area are made for a bed of spherical grains. In order to apply the formulas to all shapes we need to add a shape factor,  $C_s$ . Tests done by Douglas W. Barr show that the shape factor for a particle range from 1 - 1,35, where 1 is for spheres and 1,35 is for jagged and irregular grains. We find that that[5]:

$$S = C_s S_0 (1 - n) \quad (3.6.9)$$

However, during the Ormen Lange project in the North Sea, several experiments were done in order to determine the material flow into rock fill. They found that the pressure loss over the height of the mixed zone of clay and rocks can be determined by[10]:

$$p = s_u^* \sqrt{(n/k')} \alpha D \quad (3.6.10)$$

where  $\alpha$  is a constant between 0,6 and 0,9 with 0,75 as a good estimate, and  $k'$  is the intrinsic permeability. From this equation the surface area can be extracted as[10]:

$$S = \sqrt{n/k'} \alpha \quad (3.6.11)$$

Equation 3.6.11 has been added here as an alternative that could prove valuable in future work, but equation 3.6.9 will be the main focus when performing simulations in the theoretical model.

### 3.6.4 Diameter

Determining the right diameter to be use in a theoretical model of a porous medium is a rather difficult task. Several propositions have been made on the subject, and there seems to be many opinions as to what is more appropriate. The most convenient factor to use is the  $d_{50}$ , which is the median diameter and can be retrieved directly from a particle distribution chart. The problem with using this value, however, is that it will not represent the entire bulk of grains, and the pressure drop calculated when using it will be about 50% lower than the real value[17].

A more scientifically correct value is the sauter mean diameter, named after Josef Sauter, who first used this value in his work with internal combustion engines in 1924[23]. This diameter represents a much more advanced way of calculating a diameter that is valid for the particle distribution as a whole. The sauter mean diameter is expressed as  $d_{32}$ . The method is based on "*an estimation of the mean size of a given particle distribution. It is defined as the diameter of a sphere that has the same volume/surface area ratio as the particle of*



interest”[12]. However, this method requires advanced calculations or a diffractometer to be determined. For that reason the median diameter  $d_{50}$  will be used for the theoretical model in this paper. This is because it is more the trends and behavior of the materials that are important rather than finding an exact answer.

### 3.6.5 Determining the permeability

The Blake-Kozeny-Carman(BKC) model, which uses a packed bed of spheres to describe the flow of a fluid through porous media, is one of the most widely used in the field of fluid dynamics. Several equations have been developed separately for determining different aspects of liquid flow under various conditions. The BKC model manages to connect and implicate many of these conditions in one model. This includes the viscosity, the pressure drop over the medium, the porosity, superficial velocity, and the diameter of the particles. All of these parameters are connected in order to find the coefficient of permeability,  $k$ . The model is only valid for laminar flow, i.e., low Reynolds number ( $Re < 2$ )[17][25].

The Kozeny-Carman equation for determining permeability is derived from Pouiseuille’s formula for viscous resistance in a round conduit with laminar flow[17]:

$$\Delta p = \frac{32\eta v L}{D^2} \quad (3.6.12)$$

where  $\eta$  is the dynamic viscosity of the fluid,  $v$  is the average velocity in the conduit,  $L$  is the distance, and  $D$  is the diameter of the conduit. Hence the Kozeny-Carman assumes that the fluid flow in the pores can be compared to flow in straight circular tubes. The pressure driving the flow in the tubes is approximately equal to the viscous resistance,  $F_p = F_v$ [5], so that the driving force can be expressed as:

$$F_p = \frac{\Delta p}{L} = \frac{\rho g \Delta h}{L} \quad (3.6.13)$$

By applying equation 3.6.12 to a single pore of porous media we introduce the average pore velocity,  $v_p$ [5]:

$$\frac{\Delta p}{L} = \frac{8\eta v_p}{D^2} \quad (3.6.14)$$

Here the average pore velocity is related to the normal velocity by  $v = n v_p$ , where  $n$  is the porosity. As explained in 3.6.2, the actual length the fluid has to travel is possible to explain by introducing a factor called the tortuosity. The velocity of the fluid in the pores will also differ from the assumed straight flow, as the flow from pore to pore will be controlled by local pressures in the pore spaces[5]. Hence a a constant to regulate the velocity needs to be introduced. This constant can be expressed in terms of the length:  $v_p = v_p * (L'/L)$ .

Combining equations and introducing the constant of tortuosity from 3.6.2 we get[5]:

$$v = \frac{\rho g n m^2}{5\eta} * \frac{\Delta h}{L} \quad (3.6.15)$$

Here  $m$  is the hydraulic radius, which can be found from the average radius of the pore channel:  $m = \text{porosity/surface area}$ [5]. When comparing 3.6.15 to Darcy's formula (3.6.2) we find the permeability  $k$ :

$$k = \frac{\rho g n m^2}{5\eta} \quad (3.6.16)$$

The entire derivations of these formulas can be found in [5]. The surface area and the shape factor still need to be added into the formula. Following the procedure explained in 3.6.3, the equation for determining the permeability by using the BKC model is found[5]:

$$k = \frac{\rho g}{5\eta C_s^2 S_0^2} * \frac{n^3}{(1-n)^2} \quad (3.6.17)$$

## Chapter 4

### Laboratory experiments

This chapter gives a recollection of the experiments performed in the laboratory. Since finding clay from the bottom of the North Sea is a rather difficult task, a realistic replica had to be created. It is also difficult to find a material that matches an offshore clay in stress history, structure and organic content, hence after finding a clay that had similar properties, it would still have to be modified. The clay that was used for the experiments was found and dug up from a beach area called Leangbukta near Trondheim, Norway(4.0.1). Seeing as it was not necessary to test the clay in in-situ conditions, it was dug up with a regular shovel during low tide. The sample was taken at a depth of approximately 0,5 meters.

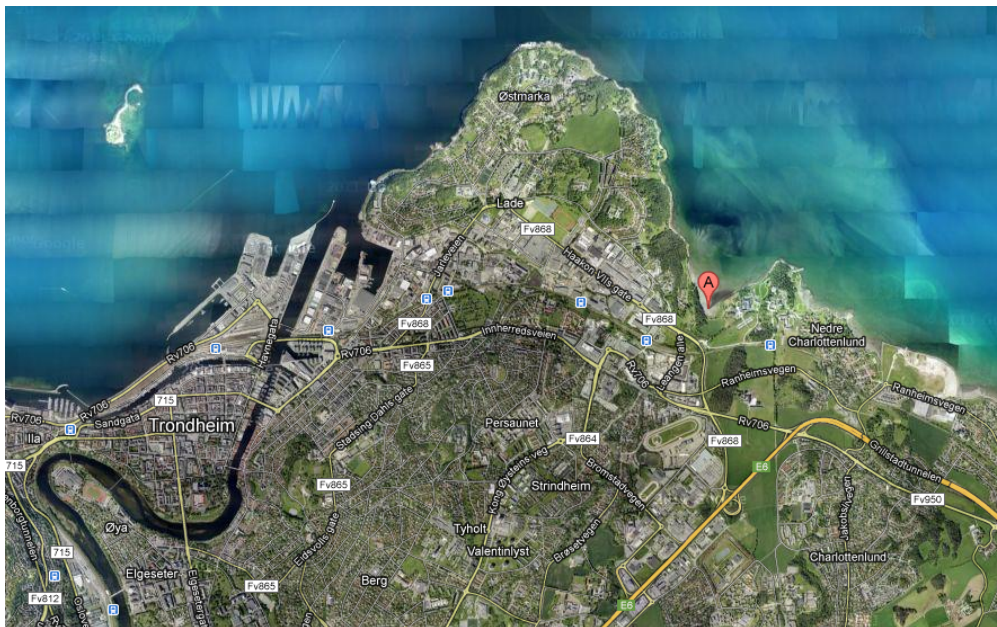


Figure 4.0.1: Leangbukta  
[13]

## 4.1 Routine parameters

Index testing had to be done on the clay in order to determine its contents and structural parameters. Parameters like the shear strength would have to be modified, and therefore not of immediate importance. What would have to somewhat coincide with an offshore clay, however, was characteristics like the liquidity and plasticity indices. Also the grain size distribution is important in this context, but it is very hard to find a clay with the same level of clay grains in the Trondheim region. Or more specifically with a low amount of silt[20]. The results from the index testing can be found in the table below(4.1).

Table 4.1: Routine parameters

Test	symbol	value
Water content	$w$	30%
Liquid limit	$w_l$	32,8%
Plasticity limit	$w_p$	20,6%
Grain density	$\rho_s$	2,94g/cm <sup>3</sup>
Plasticity index	$I_p$	12,2%
Liquidity index	$I_l$	0,77%
salt content	$S$	19g/l
Ring density	$\rho$	1,96g/cm <sup>3</sup>

A hydrometer analysis was also done in order to get the grain size distribution, and the results showed a fairly large content of silt in the clay. See the graph below(4.1.1)

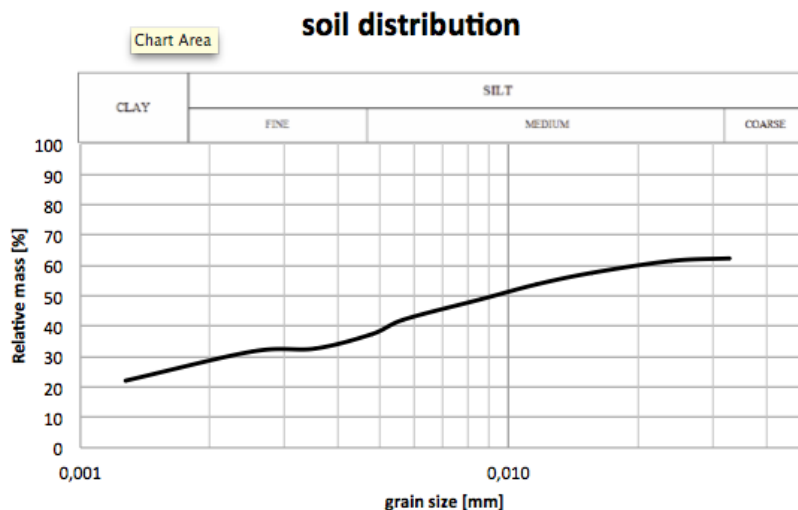


Figure 4.1.1: Grain size distribution

#### 4.1.1 Analyzing results

The material is a marine clay with a rather low plasticity index. According to the classification system for norwegian clays it is classified as a medium plastic clay ( $I_p = 10-20\%$ )[22] Because of this the clay reacts abruptly with added water and goes from more or less stable to a fluid-like behavior very quickly. The fact that the water content,  $w$ , is so close to the liquid limit,  $w_l$ , indicates that this is a material with a low shear strength[21]. The original salt content is quite low, and is probably due to groundwater from the shore mixing with the seawater. This is possible to modify, and shouldn't influence the final results of the experiment.

Samples have previously been taken from the seabed in the North Sea as a part of the investigations regarding the Ormen Lange project. The samples were taken from depths that represent before and after the Storegga slide[6], unit 2 and unit 1 respectively[7]. The clay at unit 1 should be softer than the compacted clay at unit 2 from before the slide. See table 4.2 for comparison of the material found at Leangbukta with the two soils from Storegga.

Table 4.2: Comparison with soils from Ormen Lange[7]

Test	symbol	Leangbukta	Unit 1	Unit 2
Water content	$w$	30%	60-150%	19%
Liquid limit	$w_l$	32,8%	80%	35%%
remolded shear strength	$s_r$	?	0,4-2,35kPa	5kpa
Grain density	$\rho_s$	2,94g/cm <sup>3</sup>	2,76g/cm <sup>3</sup>	2,77g/cm <sup>3</sup>
Plasticity index	$I_p$	12,2%	50%	18%
Liquidity index	$I_l$	0,77	2,0	0,3
clay content	—	30%	40-60%	40%

The water content is very different for all three soils. This is probably because the clay found in Leangbukta was not found under water, but simply taken from the shore. At unit 1 the clay is soft with a low density as this is the remains of a big slide, hence water can easily penetrate the clay. Due to this the water content is far above the liquid limit of the clay, which can be seen by the liquidity index in table 4.2. The soil at unit 2 is more compacted and therefore harder to penetrate. The water content here is well within the plasticity index. The remolded shear strength for the clay found at Leangbukta will have to be modified to fit the clays from unit 1 in particular, as this is the softer clay and more relevant for these experiments. This will be done by increasing the water content (see 4.1.2). Regarding the content of the soils, the clay from Leangbukta is more similar to the one found at unit 2. This is due to the geological conditions. They are both compacted with a higher silt-content than the soil at unit 1. This is unfortunate for the experiment, but finding an onshore clay as "fat" as the one found on the seabed is difficult.

#### 4.1.2 Water content vs. shear strength

The relationship between the water content of the clay and the shear strength at that given water content was interesting as part of finding the viscosity. Water was added to a clay mixture, and the shear strength was measured using the falling cone method. This way the water content of the clay could be predicted based on a measured shear strength. This can not be compared to an offshore clay, however, because of the salt content. With increasing salt content, we get an increased shear strength, thus there can be a higher water content with the same low shear strength with increased salt content. The results found for this specific clay can be seen below in table 4.3 and in figure 4.1.2

Table 4.3: Water content vs. shear strength

Sample	mass wet [g]	mass dry [g]	mass water [g]	$S_r$ [kPa]	w [%]
1	29,84	23,03	6,81	9	29,5
2	40,12	29,80	10,32	2,1	34
3	53,12	37,80	15,32	1,1	40
4	40,7	28,07	12,63	0,98	45
5	28,04	18,94	9,1	0,69	48
6	42,30	27,40	14,9	0,39	54

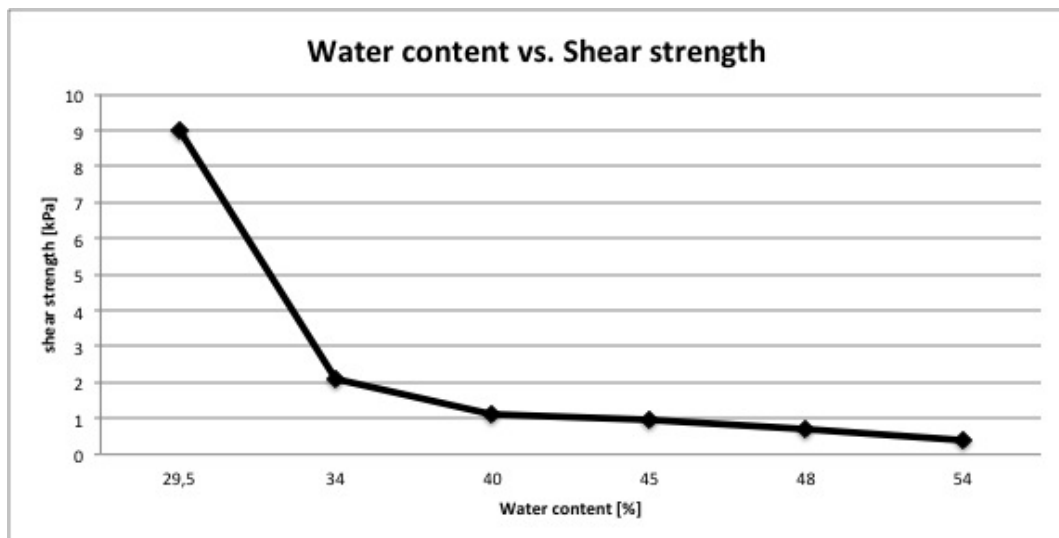


Figure 4.1.2: water content vs. shear strength

## 4.2 Finding the thixotropy

The best way to find the thixotropy is by determining it in terms of the viscosity. For that one needs an instrument capable of reading the two in relation to each other. This is explained in section 3.4 Such an instrument was not available, and the thixotropy is therefore represented in terms of how the remolded shear strength changes with time. If the material is thixotropic, the shear strength will increase with time as the structures in the clay will attempt to reform. A falling cone device was used to measure the remolded shear strength over a longer period of time. In order to prevent water to escape from the sample, a box with a lid was used to contain the material between each measurement. The results found for this specific clay can be seen in table 4.4.

Table 4.4: Thixotropy

Time	Remolded shear strength[kPa]
0min	0,29
10"	0,29
20"	0,29
30"	0,39
50"	0,39
1:10	0,39
1:40	0,39
2:10	0,39
2:40	0,39
4:10	0,49
5:40	0,49
24t	0,59

## 4.3 Description of the experiment

The experiment was constructed as a replica to simulate rocks being dropped upon an area of soft clay material. In real life this is done at an enormous scale, so in order to get a somewhat realistic situation that could fit in a lab, the experiment had to be scaled down significantly. The idea for the experiment was produced by myself with help from my advisor Gudmund Eiksund. What the experiment is trying to show is how the soft clay behaves as it is remolded by the rocks when they hit the surface. The scope is to find out if the clay develops a fluid-like behavior, and if this is the case will it influence the settlements of the rock fill, i.e., increase the settlements in addition to conventional consolidation theory? Given that the clay behaves like a liquid, this experiment will show if it penetrates the rock fill.

As the experiment will have to be done in a confined space as opposed to the seabed, which is close to infinite, the rocks can not simply be dropped into a tank. This would cause frictional forces near the walls, which again would affect the settlements of the remaining rock

fill. In order to eliminate the friction from the model, it is easier to push the clay through the rocks than the other way around. This was done by using a cylinder and a piston. The rocks were installed in the cylinder and suspended by a grid of steel wire. Water was then added to the cylinder to simulate the presence of seawater. Finally the cylinder was lowered down using weights of a known magnitude, pushing the clay into the rocks while measuring both the pressure in the clay and the deformation of the cylinder with time. The cylinder was see-through in order to be able to properly view what happens in the intersection between clay and rock.

The pressure was measured by a pressure-censor installed in the piston, and then recorded by a computer. Deformations were measured using a wire connected to the bottom of the cylinder (4.3.2), and then recorded by the same computer using a program called Labview (see figure 4.3.2c). The cylinder is made of plexiglass with a total height of 76cm and a diameter of 24cm and was found as a spare part in one of the workshops at NTNU. The piston had to be custom made in order to fit the cylinder. It was cut from PUM and made to fit exactly into the perimeter of the cylinder. A hole was drilled through the piston to make room for the pressure-censor, and the piston was then glued to a support to create some height and stability. Finding and making the components to construct the experiment as realistic as possible was a time consuming process, but the final result seems like the best solution possible with the available materials and manpower.

Assumptions made for these experiments are that the clay is a non-newtonian fluid, more precisely with a behavior similar to that of a Bingham fluid(3.3), combined with a time-dependent thixotropic behavior, and that the clay will always have a laminar flow in the cylinder.



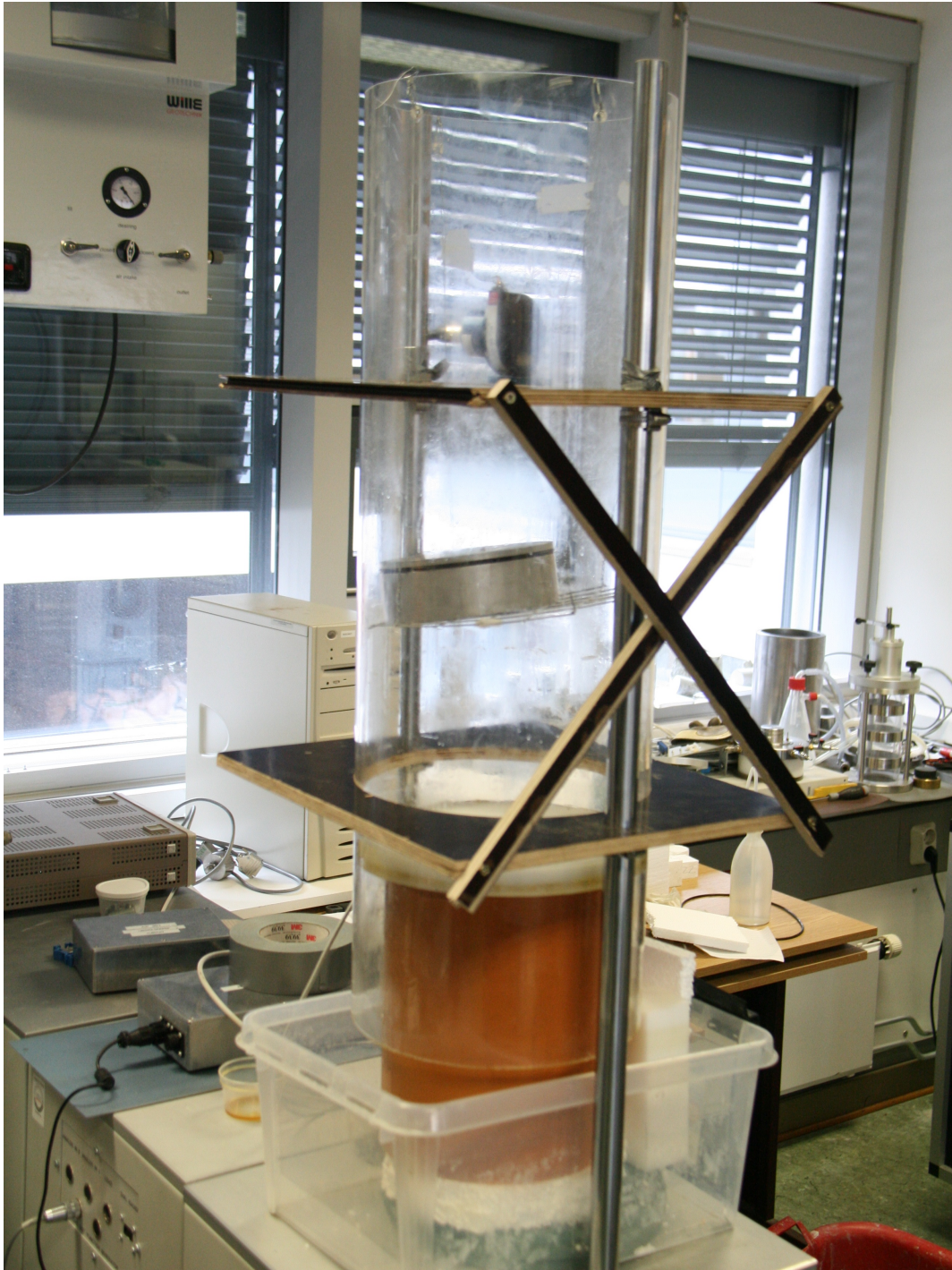


Figure 4.3.1: Empty cylinder with supports

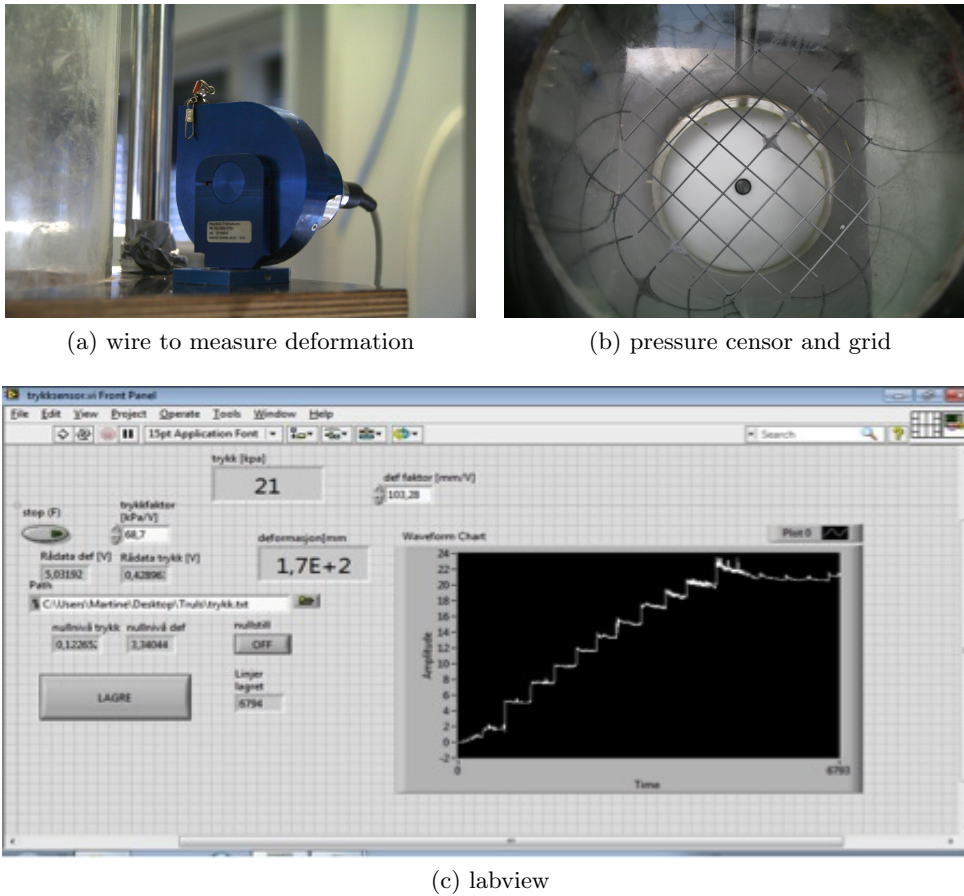


Figure 4.3.2: Devices used for measuring

#### 4.4 Experiment using Laponite

Another way to simulate the penetration of clay through a rock fill is by using a synthetic clay called Laponite. This is a transparent material that is made by mixing water with a powder. The more powder added to a fixed amount of water, the higher the shear strength of the "clay".

By adding the appropriate amount of water, it is possible to model the material to get a similar shear strength as the clay needed for this experiment. As the shear strength is the only property that is similar to the clay, the results obtained are not scientifically valid, but such an experiment can give an indication of what can be expected from the behavior of the clay. The experiment is otherwise identical to the experiment described in 4.3, however at an even smaller scale and without measuring the pressure electronically (see figure 4.4.1). This includes a smaller cylinder, and a smaller piston, which gives a more maneuverable experiment, but it will not be as realistic. What is measured is the weight used to press the cylinder down, and how far the gel penetrates the rock fill.

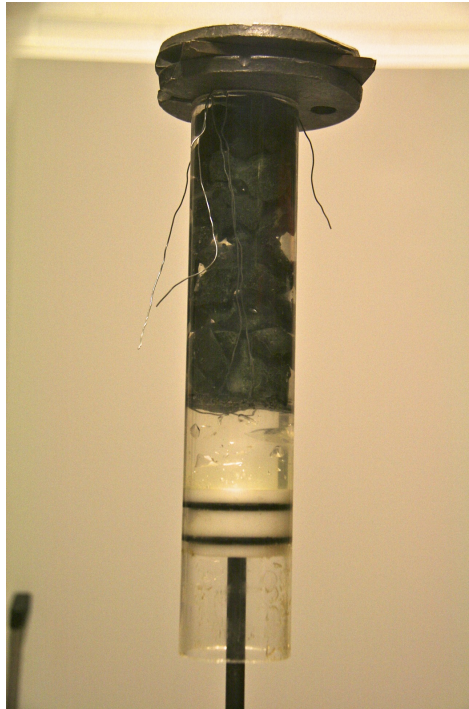


Figure 4.4.1: Experiment using Laponite

#### 4.4.1 Results and discussion, Laponite

##### Description

After experimenting with Laponite it was found that by adding the equivalent of 6% of Laponite-powder to a known volume of water, the shear strength of the Laponite-water solution is approximately 0,3kPa. This is approximately what is expected from the weakest layer of clay on the seabed. For a water volume of 1 liter, 60ml of Laponite powder was added.

The solution was then mixed for about 20 minutes at constant speed, which resulted in an almost perfectly homogenous gel. About  $240\text{cm}^3$  of laponite was added to the cylinder, which translates to a height of 10cm in the cylinder. A much smaller cylinder was used for this experiment. The rest of the experiment is described in 4.3, but this was performed without recording the data.

##### Experiment 1

The rocks used had a density of  $2,84\text{g}/\text{cm}^3$  and a void ratio of 40%. The diameter of the rocks ranged from 1-4cm. Initially 1kg was used to press the cylinder down over the piston. When the weight was first added to the top of the cylinder, the rocks were immediately pushed 3cm into the gel from the initial 10cm. After one minute the distance was 3,5cm. The settlements then came to a complete stop for about one hour. It seemed like the Laponite gel had not penetrated the rocks, but simply had been compacted by the weight. This was probably due

to air bubbles in the Laponite solution (see figure 4.4.2). These bubbles appeared during the mixing of the material. As long as there are bubbles present, they will act as a spring and farther compression seems unlikely.

As a result more weight was added, and the same result as previously occurred, with immediate settlements of 2cm, and then the movement stopped. Another possible problem is that the piston got stuck in the cylinder during the slow movement.

## Experiment 2

After the first experiment the Laponite was left untouched for about one week in order to remove some of the air bubbles in the solution. There were still some left, however, and maybe putting the gel in vacuum would give a better result. When the experiment was attempted again, the same results as before were obtained. About 1kg was added and immediately the Laponite got compressed. More and more weight was then rapidly added over a short period of time, in order to observe the effect. For each added weight (1kg each time) the rocks sank about 1cm from the initial 10cm. However, when 5kg was reached, the Laponite started to flow freely through the rock fill. If the velocity was constant is hard to predict as there were no means for measuring this. The penetration of the fluid into the rocks happened rather quickly, approximately one minute, before coming to a stop after about 8-9cm of penetration. The reason for the halt is not certain, but it probably has to do with the shear frictional force being too high due to the increasing surface area as the fluid covered more and more of the rocks, hence finding a new equilibrium.



Figure 4.4.2: Air bubbles in the Laponite

## 4.5 Experiment using clay

### 4.5.1 Experiment 1

A description of the experiment is found in 4.3. This first experiment was used more or less to get an idea of what would actually happen with the rock-clay interaction: how much weight was needed? how did the equipment and the setup of the experiment work? was the shear strength of the clay appropriate? etc. All of these questions had to be answered in this first experiment.

23cm of clay was added over the piston and the grid "basket" was set in place. The rocks were then installed. The most difficult part of the installation was to get everything to fit, i.e., get the cylinder to run smoothly over the piston with as little friction as possible, and making sure the rocks and the clay stayed in their "zero-positions" until the recording started. The steel grid worked as a support to keep everything in place. It was important for this experiment to only consider the effect of rocks sinking into the clay due to self weight. In a real situation the rock are "drilled" into the ground on impact due to the velocity they obtain as they are dropped from the ship (see section 2.2), but this part of the penetration was neglected here. For this reason the piston was pushed 15cm into the cylinder so that the clay and the rock fill were in contact before the measurements started. The weights used were regular oedometer weights with a magnitude of 10kg. They were added to simulate an increase in height of the rock fill, and to see the effect of such an increase on the clay. The equipment used can be seen in figures 4.3.2, 4.5.1, and 4.5.2. The weights added are supported by a plate at the top of the cylinder. Seeing as all the equipment had to be custom made for this experiment there is a big margin for error, and several aspects could be improved by idealizing the equipment.

The rock fill had a specific weight of  $28kN/m^3$ , which with a 40% porosity adds up to a total rock weight of:

$$m = V * \rho_r = (38 * 144\pi)[cm^3] * 2,85[g/cm^3] * 0,6 = 29,4kg \quad (4.5.1)$$

and the clay had a specific weight of  $17,1kN/m^3$ , which adds up to a total clay weight of:

$$m = V * \rho_c = (23,5 * 144\pi)[cm^3] * 1,75[g/cm^3] = 18,5kg \quad (4.5.2)$$

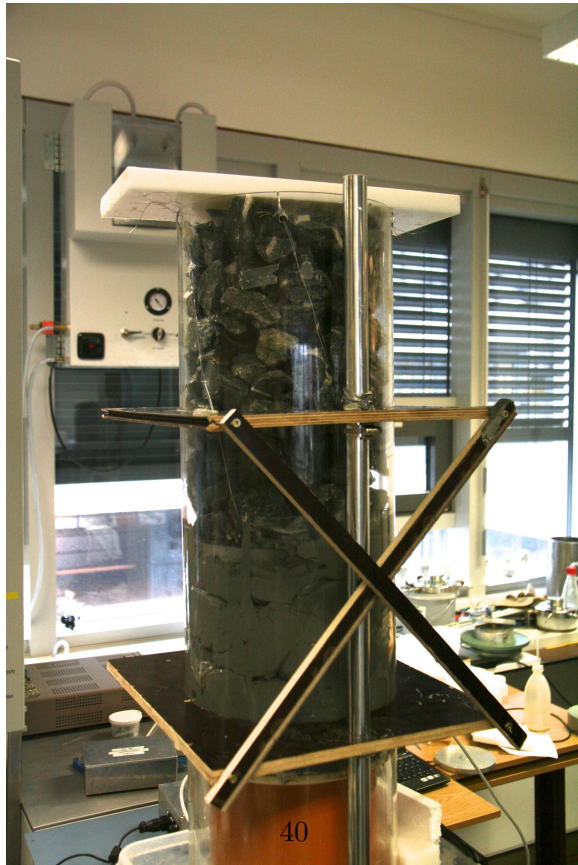
This gives a total weight of  $29,4 + 18,5 + 6,8(water) = 54,7kg$  and, in theory, an initial pressure of about:

$$\sigma = N/A = (54,7 * 9,8)[N]/0,045[m^2] = 12,0kPa \quad (4.5.3)$$

The rocks separately had a theoretical pressure on the censor of 6,4kPa.

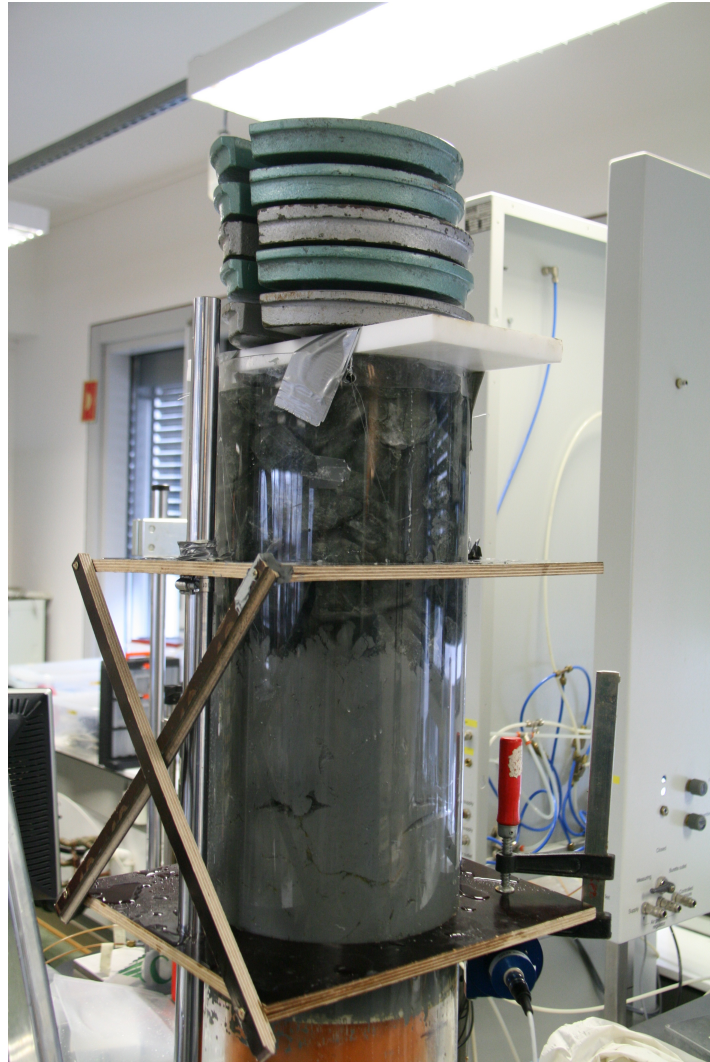


(a) Full cylinder 1



(b) Full cylinder 2

Figure 4.5.1: Cylinder filled with clay and rocks, supported by the piston at the bottom



(a) Cylinder with weights



(b) cCay flowing through rocks

Figure 4.5.2: Cylinder filled with clay and rocks, supported by the piston at the bottom

## Results experiment 1

Table 4.5: Clay data for experiment 1

Property	value
$\rho$	1,75 [g/cm <sup>3</sup> ]
$s_r$	0,78 [kPa]
$w$	44 [%]

From equation 4.5.3 we see that the initial pressure in the cylinder theoretically should be 12,0kPa. However, before removing the support of the cylinder, the initial value was zeroed out, which included everything below the steel grid, i.e., the clay and the water. This initial value was 6,8kPa, which was a bit higher than expected, but is probably caused by rocks having fallen through the steel grid, mixing with the clay prior to removing the support. Hence, an initial value of 6kPa was found when the support was removed due to the weight of the rocks. This is also a bit higher than expected ( $12,0 - 6,8 = 5,2$ ). The results are shown in figures 4.5.4 and 4.5.7.



Figure 4.5.3: Pressure with time



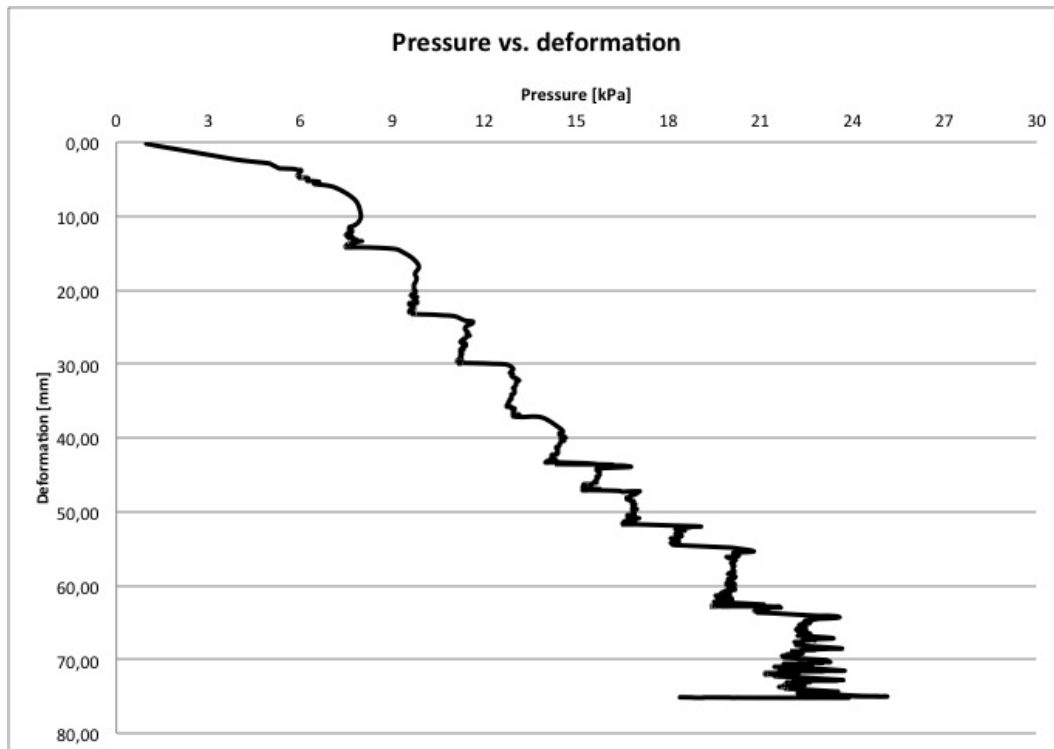


Figure 4.5.4: Pressure vs. deformation

### Discussion experiment 1

Figure 4.5.3 shows the pressure added to the system over time. Adding 10kg should give an increase of 2,1kPa on the system, but the graph shows that with increasing weight the pressure does not increase accordingly. For the first part the results are consistent and show a regular pattern. Towards the end of the experiment, adding weight gives an immediate increase in pressure, only to decrease over the next seconds. The pressure also "skips" up and down without adding weight, giving an irregular pattern.

Figure 4.5.4 shows the same pressure, but in relation to the deformation. The deformation is rather consistent in its response to the pressure. In most cases it shows the same deformation with added weight (about 5-6cm). Only in cases where the weights have been added too quickly, not allowing the deformation to "settle", the deformations are lower (about 4cm). Only towards the very end the deformation stops reacting to the increase in weight.

As mentioned in paragraph 4.5.1, experiment 1 was used to retrieve valuable information about what would actually happen in the interaction between soft clay and a rock fill, and if the experiences with Laponite proved to be similar for clay. The results were somewhat mixed. The fact that the clay penetrates into the rock fill definitely happens, but for experiment 1 this was a slow process, only depending on the amount of pressure put on the clay. The results from the Laponite experiments showed that after a certain magnitude of

pressure, the material would rapidly penetrate the rock fill(4.4.1). This did not happen here, and it is not certain whether it was the fact that more pressure was needed for this to happen, or if other unknown factors prevented the clay from flowing. It seems like the piston may have been unlevelled in the cylinder towards the end of the experiment, making it close to impossible for the piston to move farther. If this was the case, it would have reduced the deformations greatly. The unstable piston was probably caused by the styrofoam-support that was used, as a hard surface is crucial as support for the piston.

Another aspect is that the porosity may have been smaller than assumed (40%), and thereby affecting the permeability of the rock fill. This would decrease the cross-sectional area of the "tubes" mentioned in chapter 3, and following the Kozeny-Carman equation(3.6.17) it would make it harder for the clay to flow.

The clay may also have been too hard with its shear strength of 0,78kPa and a softer clay could prove to be give more satisfactory results. Because the weights were put down with intervals of several minutes, the shear strength may have been increased due to thixotropy. The thixotropic results for this clay 4.4 show that the shear strength will increase rather rapidly with time. As the experiment was done in a "start and stop" motion, parts of the clay may have had problems "starting up" again due to this phenomenon.

#### 4.5.2 Experiment 2

The second experiment was done with the same equipment and materials as the first, see figures 4.3.2, 4.5.1, and 4.5.2, and following the same procedure for the setup of the equipment as was explained in 4.5.1. Differences in experiment 2 consisted of the water content in the clay being higher in order to get a softer material (shear strength of 0,35kPa), and the support for the piston was substituted as can be seen in figure 4.5.5. The reason for the new support was that this one was higher, producing slightly more leverage for the amount of clay in the cylinder. This support was also more stable so that the piston would not "twist" inside the cylinder. Figure 4.5.5 also shows how a tube was added to the system to control the flow of water.

The clay was made softer in order to improve the chances of producing the wanted effect, namely that the clay would flow into the rock fill. The shear strength of 0,35kPa was more similar to the shear strength of the Laponite ( $\approx 0,3\text{kPa}$ ) (4.4.1). Besides from that, experiment 2 was done very similarly to experiment 1. The main difference in the procedure was that the weights were put down with a more set time interval (about 8 minutes), where in experiment 1 they were loaded more arbitrarily.

The weight of the rocks was the same as for experiment 1 (see equation 4.5.1), namely 29,4kg. The clay had a different density ( $1,7\text{g}/\text{m}^3$ ), which with a height of 24cm gives a weight of:

$$m = V * \rho_c = (24 * 144\pi)[\text{cm}^3] * 1,7[\text{g}/\text{cm}^3] = 18,5\text{kg} \quad (4.5.4)$$

This turns out to be the same as for experiment 1 (4.5.2), giving a total theoretical weight of:

$$m = 29,4 + 18,5 + \text{water} = 47,9\text{kg} + \text{water} \Rightarrow 10,5\text{kPa} + 1\text{kPa}(\text{water}) = 11,5\text{kPa} \quad (4.5.5)$$

There was also less water in the cylinder during this experiment in order to have better control of the system.

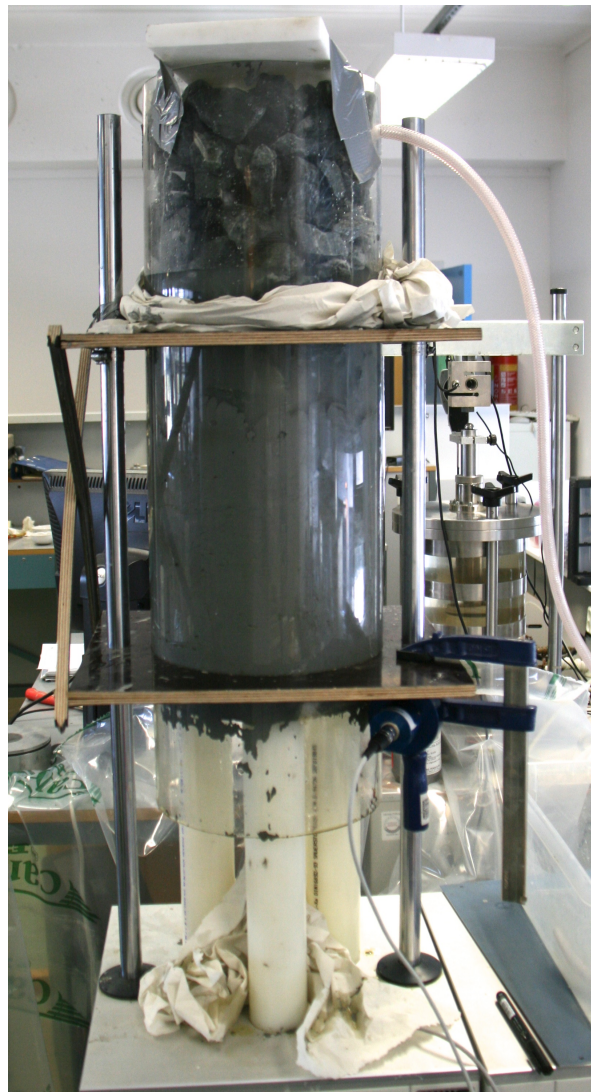


Figure 4.5.5: New support for the cylinder

## Results experiment 2

Table 4.6: Clay data for experiment 2

Property	value
$\rho$	1,7 [g/cm <sup>3</sup> ]
$s_r$	0,35 [kPa]
$w$	52 [%]

The theoretical pressure for the clay alone was 4,02kPa based on the measured values for density, 1,7g/cm<sup>3</sup>. However, the pressure-censor at the bottom of the cylinder measured an initial value of 3,7kPa. This was "zeroed out" before loading the rocks and the water. Before the support was removed the censor indicated that the rocks influenced the clay by 0,8kPa and an initial deformation of 1,2mm. With added water the pressure rose to 1,7kPa. When the support was removed the pressure immediately increased to 5,2kPa with a deformation of 20mm. Weights were then added with approximately 8 minute intervals. The results can be seen in figures 4.5.6 and 4.5.7. The total deformation is about 175mm at a pressure of almost 21kPa.



Figure 4.5.6: Pressure with time 2

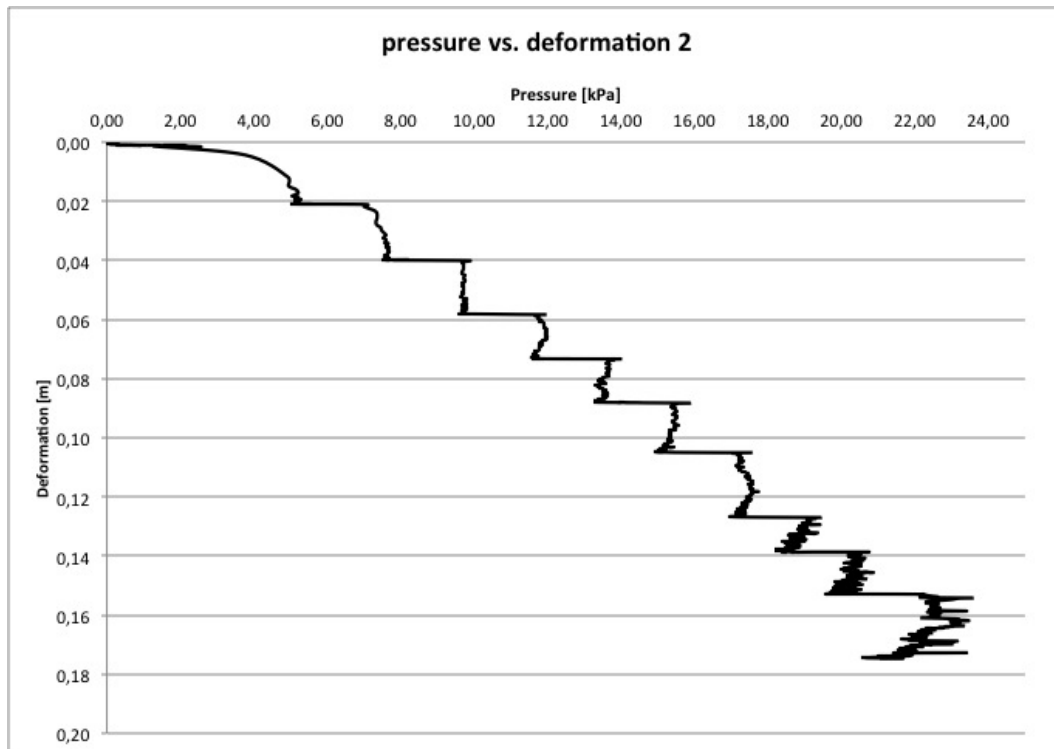


Figure 4.5.7: Pressure vs. deformation 2

### Discussion experiment 2

The reason for the theoretical value for the pressure in the clay being higher than the actual measured value could simply be due to air bubbles in the clay. There is a lot of water in the clay (52%), hence there is most likely also a lot of air contained in the material. This will make the clay "lighter" than the calculated value. Figure 4.5.6 shows a slight increase in pressure from 0 - 1,7mm. This is because recording was started before loading the rocks into the cylinder, and this increase is just due to adding the rocks. The rocks should initially not influence the pressure before the support for the cylinder was removed, but as the clay went slightly over the grid, the rocks applied some pressure to the clay. From figure 4.5.6 we see that the pressure increases consistently with each load step ( $10kg = 2,16kPa$ ). Figure 4.5.7 shows the deformation versus the pressure, and from the graph we see the same trend: that the deformation is consistent with each added load step (about 20mm), although more pronounced in the beginning than towards the end. In the beginning we have a sort of "start-and-stop" motion, while approximately halfway through the experiment it seems like the movement never really stops. The motion get slower with time, but it does not stop, and the velocity increases with added load. Nor are the deformations as big towards the end of the experiment. The same phenomenon occurred when laponite was used and is most likely due to the fact that as more clay penetrates the rock fill, the surface area that the clay covers

will increase, and hence increasing the frictional force due to shearing.

Both figures show that this experiment was more successful than the first, but the stabilization-plates on the outside of the cylinder may have caused some friction, and although it may not have been significant, some energy was most likely lost to these frictional forces.

The whole process of the clay moving through the rocks was rather slow. In order for the clay to reach the top of the cylinder, almost one and a half hour was needed. It was clear during the experiment that the flow of clay chose the "easiest" path through the pores of the rock fill, forming "channels" or "rivers" of clay. This effect could be due to thixotropy. During the intervals between each load step, the shear strength of the clay would have had time to increase, making it harder for the flow to restart due to frictional forces. The clay would also have time to stick to the rocks by cohesion in the clay, or suction due to capillary bonds between the rocks and the clay. This would create barriers that would reduce the permeability.

The fact that less water was added in this experiment should not have a significant effect. Although both the clay and the rock fill will be submerged in water in a real-life offshore condition, it is difficult to replicate this phenomenon in the lab. This would have to include much more pressure on the actual water in the cylinder. The idea of the water in these experiments was mainly to make sure that the rocks were wet so as to not contribute to increased friction.

### 4.5.3 Experiment 3

This experiment was conducted somewhat different to the two previous ones. In this experiment the main interest was to study the effect of loading the entire weight immediately (or at least very rapidly). Experiment 3 was set up in the exact same way as experiment 2, using the same support and the same water content, and hence also the same shear strength in the clay. The only minor difference was that the height of the clay was slightly lower, which gave a total weight of the clay:

$$m = V * \rho_c = (23 * 144\pi)[cm^3] * 1,7[g/cm^3] = 17,7kg \quad (4.5.6)$$

giving a theoretical initial clay-pressure of:

$$\frac{17,7[kg] * 9,8[N]}{0,045[m^2]} = 3854Pa = 3,85kPa \quad (4.5.7)$$

As perviously mentioned the aim for this experiment was the same as before, but here all of the weights (almost 100kg) were added in rapid succession immediately after removing the support. As no machinery was available for loading the weights, it had to be done manually. For this reason the weights were added one by one, 10kg each time, with an interval of a few seconds. A video was taken of this. The idea behind the experiment is that by adding the

weights rapidly the thixotropic effect would not influence the shear strength, and by keeping the motion and shear rate constant, the viscosity would increase rather than decrease, and would not to surpass the yield point of the clay for each load step (3.2.4), assuming that the clay behaves like a Bingham fluid (3.3).

### Results experiment 3

Table 4.7: Clay data for experiment 3

Property	value
$\rho$	1,7 [ $g/cm^3$ ]
$s_r$	0,35 [ $kPa$ ]
$w$	52 [%]

The clay-properties were the same for experiment 3 as for experiment 2, but as slightly less clay was added to the cylinder, the initial theoretical pressure was 3,85kPa (4.5.7). Similarly to experiment 2 the actual measured value was less than the theoretical value, namely 3,3kPa, measured in Labview. This value was "zeroed out" before water and rocks were added to the cylinder. This time the rocks did not influence the pressure in the clay as there was no contact between the two prior to removing the support for the cylinder. With added water, however, and including the top plate, the starting pressure for the experiment was 1kPa with a deformation of 0,2  $\approx$  0mm. As soon as the support for the cylinder was removed the clay rose almost 50mm into the rock fill, before coming to a stop similar to the previous experiments. This can be seen in figure 4.5.8. The weights were then added in rapid succession, 10kg at a time, with a total weight of 100kg. As the weights were added one by one, the graph in figure 4.5.9 shows a jagged line between 140-190 seconds. The pressure at this time increases from 5kPa to almost 25kPa with the deformation going from approximately 50mm to 200mm.

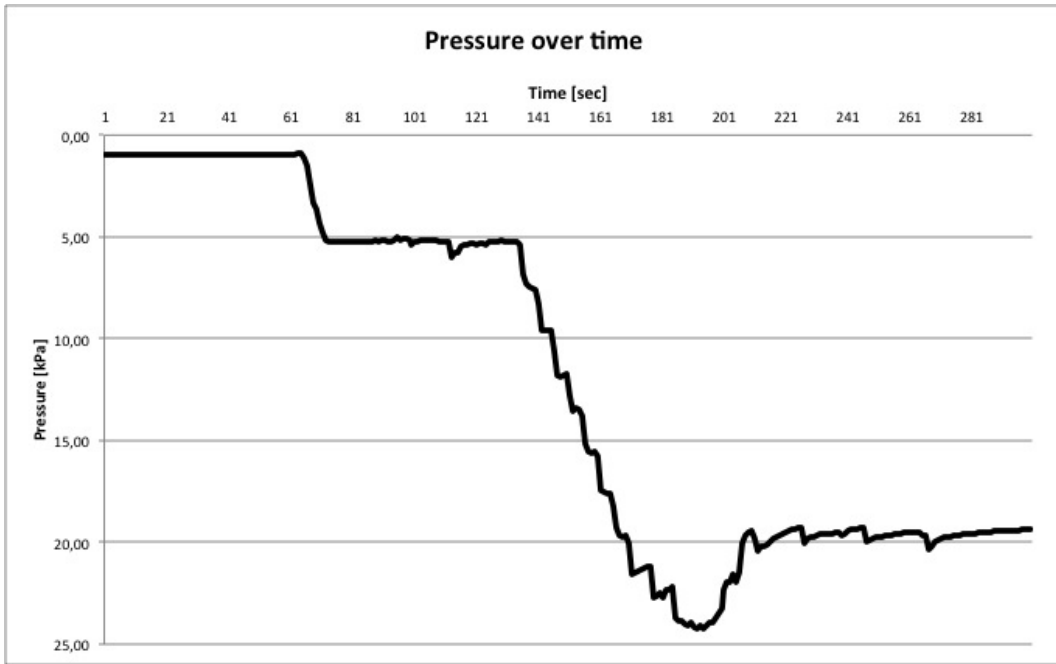


Figure 4.5.8: Pressure with time 3

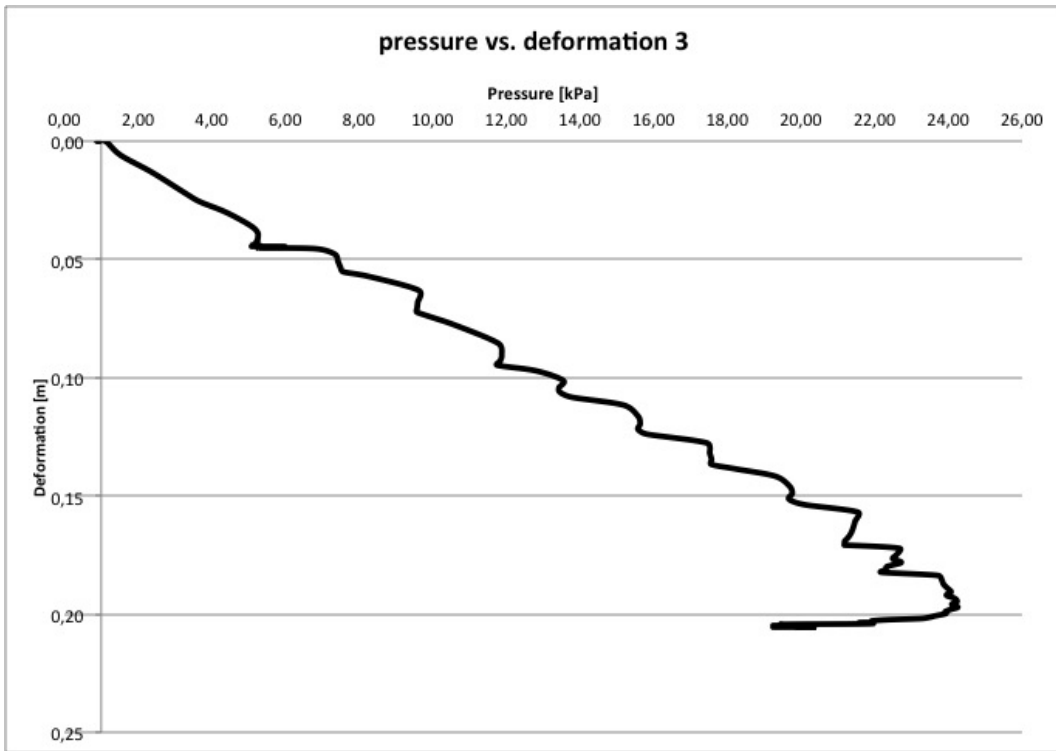


Figure 4.5.9: Pressure vs. deformation 3



### Discussion experiment 3

Both the pressure and the deformation reached a higher level in this experiment compared to experiment 2 (25kPa and 200mm for experiment 3; 21kPa and 175mm for experiment 2). The entire deformation is also a lot shorter in experiment 3. The whole experimental process was done in less than one minute compared to over one hour in experiment 2. This is probably caused by several aspects:

By loading rapidly the clay will not have time to increase its shear strength with time (thixotropy) because the movement never stops, refusing the structures in the clay the possibility or time to reform. This way the entire cross section of the clay will flow as one big mass with an approximately constant velocity and constant shear rate. In the previous experiments the clay moved in "channels" formed by the easiest or quickest way through the rock fill.

Another aspect that influenced this rapid movement is the viscosity. Again assuming that the clay behaves like a non-newtonian fluid, or more specifically a Bingham fluid, the material will have a yield point in terms of its viscosity or resistance to flow. Once passing the yield point, the viscosity will decrease with an increased shear rate, but by keeping the shear rate constant the viscosity will also be constant. Nor would the clay have had time to stick to the rocks while passing them due to the velocity of the movement, not allowing capillary bonds to form and thus preventing suction.

### Conclusions to the experiments

These experiments show that the speed at which the load is applied will be a big contributing factor to the velocity of the flow in the rock fill. When comparing experiment 3 to experiment 2 the total settlements caused by the weight of the rock fill were less when the load was added over a longer period of time. Figures 4.5.7 and 4.5.9 also show that the magnitude of the load applied is not important in regards to the settlements. Relatively the rock fill will sink just as much with a height of 0,5m as with a height of 2m. If anything, the relative settlements are less with increased height of the rock fill due to frictional forces as more surface area is covered.

It seems like the experiments are showing different viscosities for the clay depending on the speed at which the loads are applied. The settlements in experiment 3 are extremely quick in comparison to the the other two experiments, from which can be concluded that the viscosity or the viscous behavior must be different, i.e., experiment 3 shows a lower viscosity. Seeing as the settlements happen over such a short period of time, the thixotropic effect will be minimal, keeping the viscosity close to constant for experiment 3. The settlements reach more or less the same level, but the relative velocity of the clay movement at which the settlements happen is much higher with a shorter load-step interval. However, for these experiments the shear strength of the clay was consistent throughout the material. It is likely that on the seabed the shear strength will increase with depth. If the rheological behavior of the clay stops at a certain shear strength, this would cause the rock fills to stop at the the

not only a higher level, but also at a more consistent level independent of the height of the rock fill.

#### 4.6 Finding the viscosity

There are several ways of measuring the viscosity of a fluid. The most straightforward method is probably to use a flow cup, also known as an efflux viscosity cup. This is a standardized device designed specifically for measuring the viscosity. One simply fills the cup with the fluid and measures the time it takes for everything to drain through a hole in the bottom. There are several types of cups with different dimensions, but the most common is the one called ISO 243[18]. The output of this device is a singular value for the viscosity.

A more advanced method for measuring the viscosity is by an oscillatory test, which can be used on all kinds of viscoelastic materials. The most simple of the oscillatory tests is the two-plate model, which will be used to explain the principle of the test (see figure 4.6.1a): The liquid is placed between two plates where oscillations of the upper plate is produced by using an eccentrically connected rod. When the rod is turned the upper plate with a certain area is moved back and forth while the lower plate is rigid[18]. Two conditions have to be met in order for the test to be valid[14].

1. Connection between the sample and the plates has to be fixed, i.e., no sliding along them.
2. Deformation of the sample must be homogeneous over the entire shear gap.

The complex viscosity  $\eta^*$  is then found from the equation:

$$\eta^* = \frac{\tau}{\dot{\gamma}} \quad (4.6.1)$$

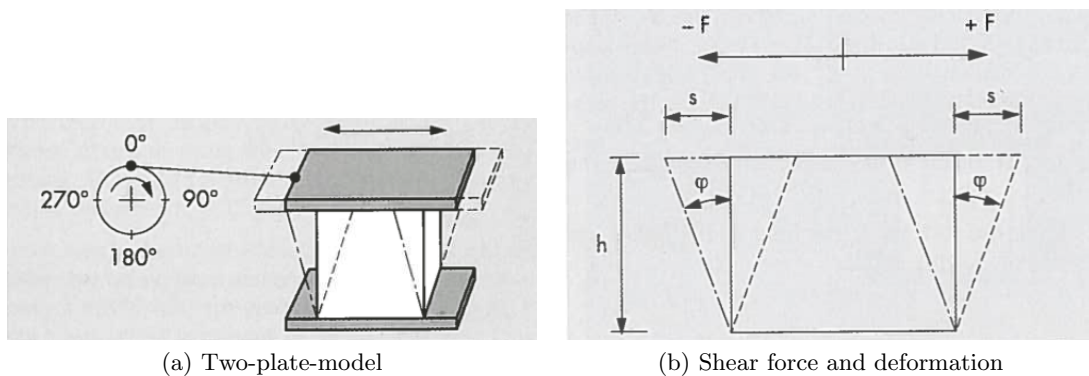


Figure 4.6.1: The two-plate model and a visualization of the shear force and deformation

Oscillatory tests can be divided into controlled shear strength (CSS) and controlled shear

rate (CRS) tests. Choosing one or the other is determined by the type of liquid in question and what you want to find from the experiment. The CRS test is most appropriate when one wants to simulate specific flow velocities. CSS is better when one wants to simulate flow or creep that is dependent upon an acting force, e.g., a river or an avalanche [14]. By controlling the shear stress or the shear rate the test can produce several values for the viscosity and the flow, and then plot the results in charts to make flow and viscosity curves (see figure 3.2.1).

For the experiments in this report the ideal method for measuring the viscosity would be by using a rheometer. This is a device that only requires a small amount of fluid, in this case clay, and uses an extremely exact oscillatory test based on a rotational disc, which can be seen in figure 4.6.2. The rheometer produces very accurate flow and viscosity curves also at slow speeds. This makes it possible to determine an accurate yield point of the liquid, as well as an exact viscosity. The device was available at SINTEF Byggforsk, but due to high costs and busy schedules the plans had to be dropped. However, this device is certainly something that would improve the quality of the experiment.

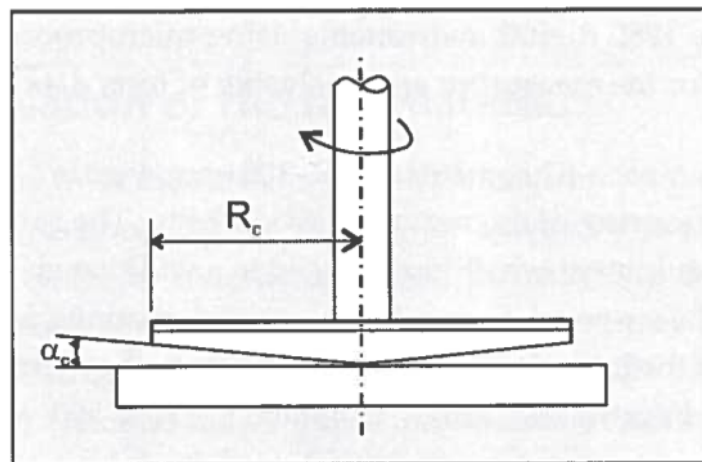


Figure 4.6.2: The cone and plate oscillatory measuring system

Another way of performing viscosity measurements is by using a viscometer. One specific kind of viscometer is called ConTek, and is mainly used to find viscosities in concrete. Such a viscometer is available in the concrete lab at Materialteknisk at NTNU. The procedure is a rotational test, which measures the torque in relation the rotational velocity of a cylinder. The output is given as a curve. This machine requires approximately  $2dm^3$  of clay. The problem with this device is that measurements at very slow rate of shear are rather inaccurate, meaning that finding the yield point of the fluid is uncertain.

#### 4.6.1 Viscosity measurements using a ConTek viscometer

Finally the ConTek viscometer described above was used to find the viscosity. The machine consists of a cylinder that is placed on a rotational disk, and another smaller cylinder, called

a beater, which contains several long blades. The measurements are performed by lowering the blades into the fluid, in this case a clay. The blades are then stationary while the larger cylinder rotates around the beater. The torque is measured in the blades and then logged by a program designed in Labview. Figure 4.6.3 shows a picture of a viscometer. This is not exactly the same as the one used for these tests, but it is very similar and the principle is the same.



Figure 4.6.3: Viscometer  
[9]

The clay is put in the bottom cylinder and the height of the clay is measured. This is the inner cylinder height. The dimensions of the cylinder are standard, and already included in the software. This includes inner and outer radius of the cylinder. For these tests a prefixed program originally made for concrete was used. The program was set to start at a certain rotation velocity as the beater was lowered, and consisted of 5 steps of different rotational velocities during which several values were logged. The output value was an average of each step.

A graph of the program, duration of each step, and rotation velocity can be seen in figure 4.6.4. For my test the max and min velocities were 0,6 and 0,1 rotations per second [rps], and the 5 steps ranged between these values. Figure 4.6.4 also shows that each step is divided into transient and sampling intervals. This is used in order for the clay to be rotated and "get used" to the specific rotation velocity during the transient interval before logging values during the sampling interval.

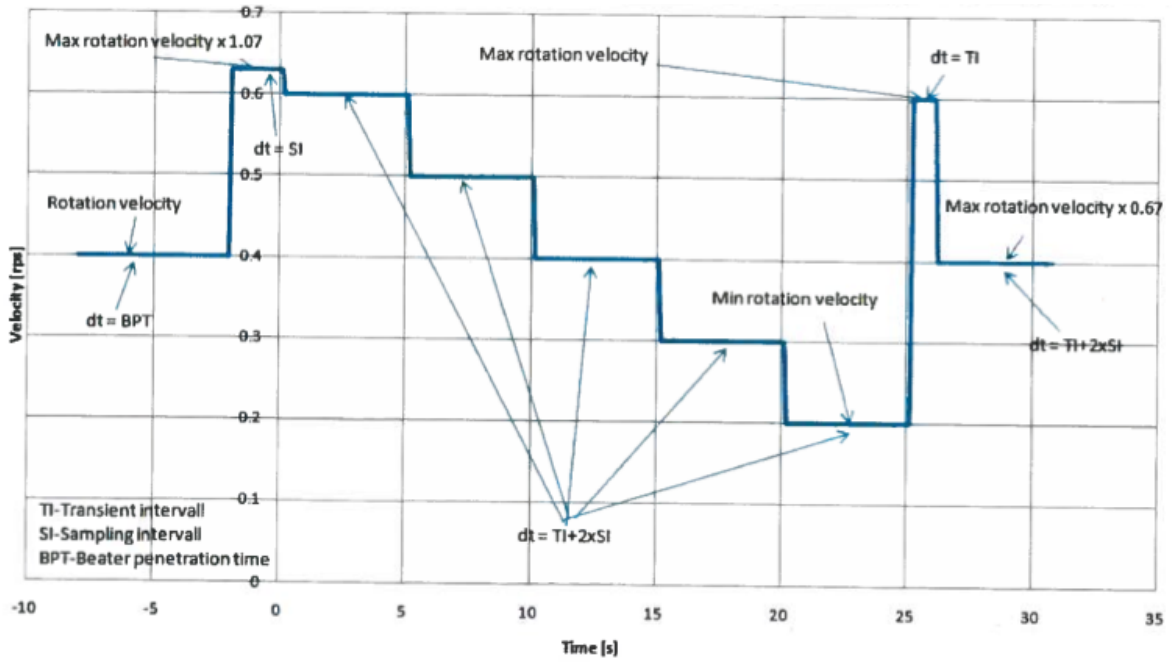


Figure 4.6.4: Setup used in program to find viscosity [4]

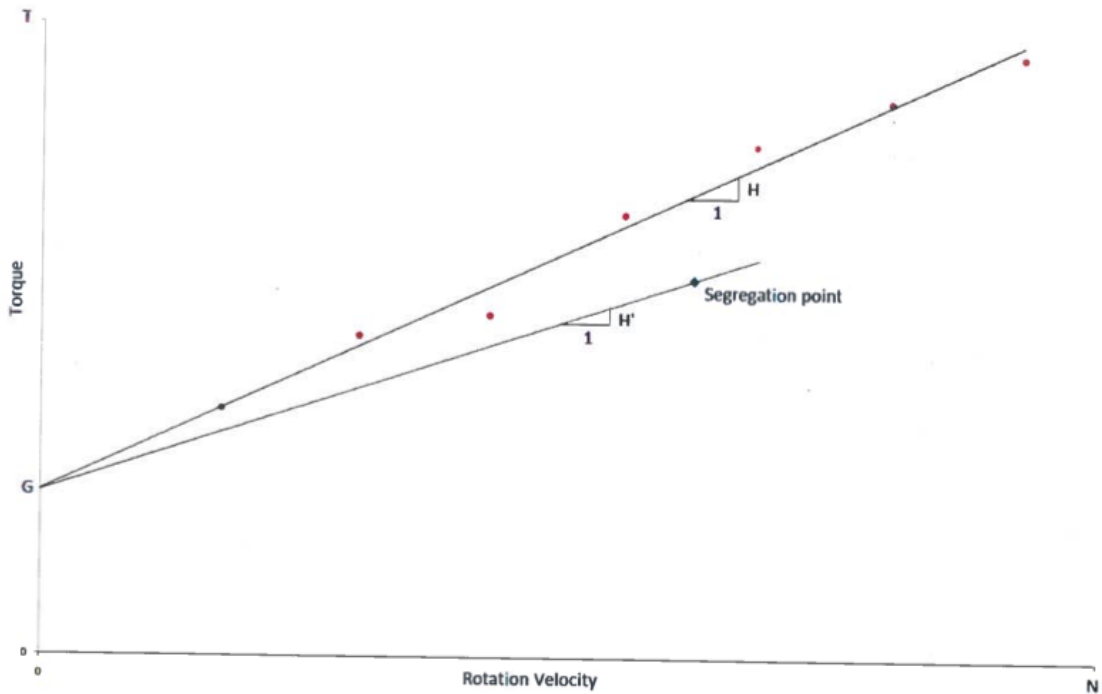


Figure 4.6.5: Example of a graph produced by a viscometer [4]

In figure 4.6.5 we can see an example of the output data retrieved from the test. The torque in Nm is plotted against the rotation velocity in revolutions per second [rps]. At the point where the fitted line intersect with  $rps = 0$  we get the flow resistance,  $G$ , as a moment. This value is used to find the yield point through the formula[4]:

$$\tau_0 = \frac{G(\frac{1}{R_i^2} - \frac{1}{R_o^2})}{4\pi h_i \ln(\frac{R_o}{R_i})} \quad (4.6.2)$$

Where  $R_i$  is the inner radius,  $R_o$  the outer radius, and  $h_i$  is the inner height of the cylinder.  $H$  is in figure 4.6.5 given as the inclination of the line. In this report this inclination value is called  $h$ , and  $H$  is used as a torque-angular dependence related to  $h$  by[4]:

$$h = 2\pi H \quad (4.6.3)$$

Finally the viscosity  $\eta$  can be found from the formula[4]:

$$\eta = \frac{H(\frac{1}{R_i^2} - \frac{1}{R_o^2})}{4\pi h_i} \quad (4.6.4)$$

## Results from viscometer test

Table 4.8: Values obtained from viscometer test

Radius inner cylinder [m]	$R_i$	0,085
Radius outer cylinder [m]	$R_o$	0,1
Height inner cylinder [m]	$h_i$	0,06
Flow resistance [Nm]	$G$	4,8
Relative viscosity[Nms]	$h$	0,957
Torque angular dependence[Nms]	$H$	0,152
Yield value [kPa]	$\tau_0$	1,5
Dynamic viscosity [Pas]	$\eta$	7,8

The output from the test are given as a text file where all the data have been automatically calculated. The graph was then produced in Microsoft excel using the data output from each step. The value at the lowest shear rate,  $rps = 0,1$  has been neglected as this value was not consistent with the other results, and knowing that the viscometer is inaccurate at low velocities, this value was left out.

Table 4.9: default

Torque [Nm]	Rotation velocity [rps]
5,429	0,608
5,173	0,480
5,225	0,353
5,010	0,225
5,296	0,405

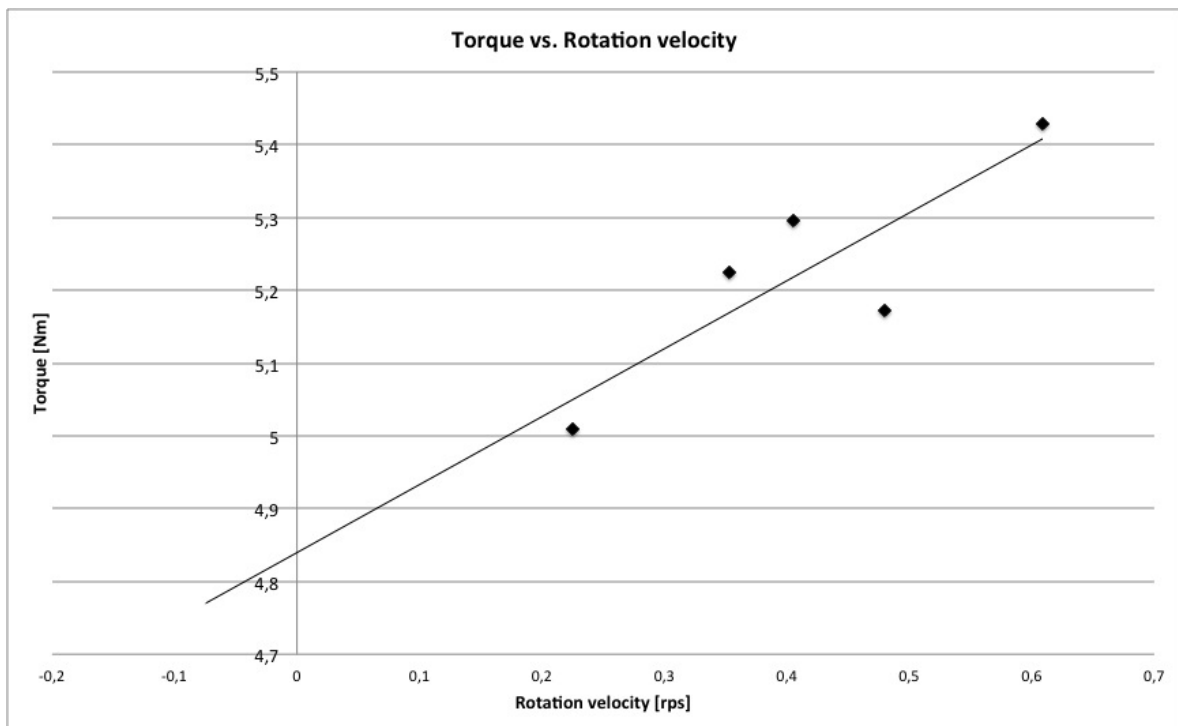


Figure 4.6.6: Torque vs. rotations velocity with fitted line produced by viscometer

## Discussion

The viscosity value,  $\eta = 7,8Pas$ , retrieved from the viscometer was in the expected range by using the experiments as a reference point, and will work as a good base when simulating the experiments in the worksheet calculation model. However, for a thixotropic fluid the viscosity will decrease with constant shear rate over time, and using one singular value for the viscosity in a material could be inaccurate if the velocity of the movement is not kept constant.

The yield value, however, is higher than what was expected. The shear strength of the clay used in the experiments and in the viscometer tests was 0,35kPa, while the yield value was as high as 1,5kPa. This is most likely due to the inaccuracies in the measurements at low shearing rates in the viscometer. When the rotation velocity is low ( $rps \leq 0,1$ ) the velocity is not consistent, and starts to "skip" up and down. The yield value should rather be measured with a rheometer for a more accurate result.



## Chapter 5

# Theoretical simulation model

### 5.1 Description

The worksheet simulation model was initially created by my advisor Gudmund Eiksund for the ormen lange project, and includes several parameters from rheology mixed with conventional geotechnical parameters. The idea is to find a relationship between the two fields, as the clay material will behave like a fluid and hence obtain rheological properties. The focus will be on finding the connection between clay properties like the shear strength and viscosity, and rock properties like the permeability and surface area. The theory behind the rheological parameters can be found in chapter 3. The aim will be to see if by determining the rheological parameters, it is possible to give an approximation of the settlements due to the clay penetrating the rock fill.

### 5.2 Parameters, descriptions and empirical values

**n**

This is the porosity of the rock fill. See 3.5 for full description. When rocks are dropped from a distance they tend to for a porosity of 0,4 or 40%. As the rock fills in question are dropped from the fall pipe of a ship this will be the value used in the worksheet.

**$d_{50}$**

The average diameter of the individual grains in the rock fill can be found in several ways, some more accurate than others. In 3.6.4 the reason for choosing  $d_{50}$  as average diameter has been described. For the experiments in this report the rocks where graded from 1-3 inches, or 2,5-7,6cm. Seeing as the majority of the rocks were of a smaller size, the diameter was estimated to be 4cm or 0,04m.

**$k'$**

The intrinsic permeability is independent of the fluid used to measure it. However, according to [10], with an average diameter of 0,04m and a porosity of 0,4, the intrinsic permeability can be estimated to  $2x10^{-6}$ .

**k**

The permeability is measured using the Kozeny-Carman equation, described in 3.6.5. This formula includes the tortuosity (3.6.2), which is a constant with a value of 5, and the shape factor 3.6.3, where a constant of 1,2 is the best estimate for this particular rock fill. It is also dependent on the viscosity and will therefore vary with the shear strength, water content, surface area, and porosity.

**S<sub>0</sub>**

As explained in paragraph 3.6.3 the model contains two methods for determining the surface area of the rock fill. One of the methods was developed for the ormen lange project [10] and includes the intrinsic permeability (3.6.10). The other method is given in [5] and includes shape factor and the average radius given from the average diameter(3.6.9). The second method has been used in the simulations, but the first method has been added as an alternative.

**density**

Several material densities are given in the worksheet based on different conditions, including the normal density for the clay, and the specific weight of the rocks mixed in both clay and in water. The clay density is here 16,6kN/m<sup>3</sup>, the density of rocks in water is 9,1kN/m<sup>3</sup>, and for rocks in clay 5kN/m<sup>3</sup>. The data for the rock densities have been chosen based in experiences and are not scientific.

**η**

In order to fit the simulations to the experiments, the viscosity will have to be iterated to get the best match possible for the curves from the experiments and simulations. For the simulation of experiment 2 a viscosity value of 40Pas was used and for the simulation of experiment 3 a viscosity of 7Pas was found to create the best match. The viscosity was also found using a ConTek viscometer in order to get the "real" value for the clay. This value was found to be 7,8Pas.

### **5.3 Construction**

The basis for the worksheet was constructed by my advisor Gudmund Eiksund. Most of the formulas are based on his experiences and previous knowledge, and some formulas have been retrieved from ormen lange [10], e.g., the formula for the surface area (3.6.10). The model is constructed so that the mean shear strength, shear force, or frictional force, and bearing capacity of the clay can be calculated with depth. These, together with the permeability and the viscosity, form the base when measuring the velocity at which the rocks travel through the soft material. The mentioned velocities are calculated for each load step based on time. In other words, the given load steps can easily be changed depending on the nature of the experiment. The loading is given in terms of the effect of applying one specific height of rock

fill, e.g., 0,6 meter or 2,3 meters, but also calculates the effect of applying the rock fill in layers, i.e., 0,6 through 2,3 meters at specified time intervals. The velocity is calculated from the formula:

$$v = k * \frac{\gamma_{rv}(H_r - H_{mix}) + H_{mix} * \gamma_{rl} - F_s - q_v}{H_{mix}/\gamma_l} \quad (5.3.1)$$

where  $\gamma_{rv}$  is the rock specific weight of rock in water,  $\gamma_{rl}$  is the specific weight for rock in clay, and  $\gamma_l$  is the clay' specific weight.  $H_r$  is the height if the rock fill.

Next calculations are carried out in the same manner for the height of the mixed zone of rocks and clay material, and for how this parameter changes with time for a given load. From this it is also possible to calculate the settlements of the rock fill due to clay penetration by using the formula:

$$settlements(\delta) = H_{mix} * n \quad (5.3.2)$$

Finally, all the parameters are gathered and compared in graphs that respond to changes in the input parameters. These can selectively be further compared to graphs obtained by performed experiments.

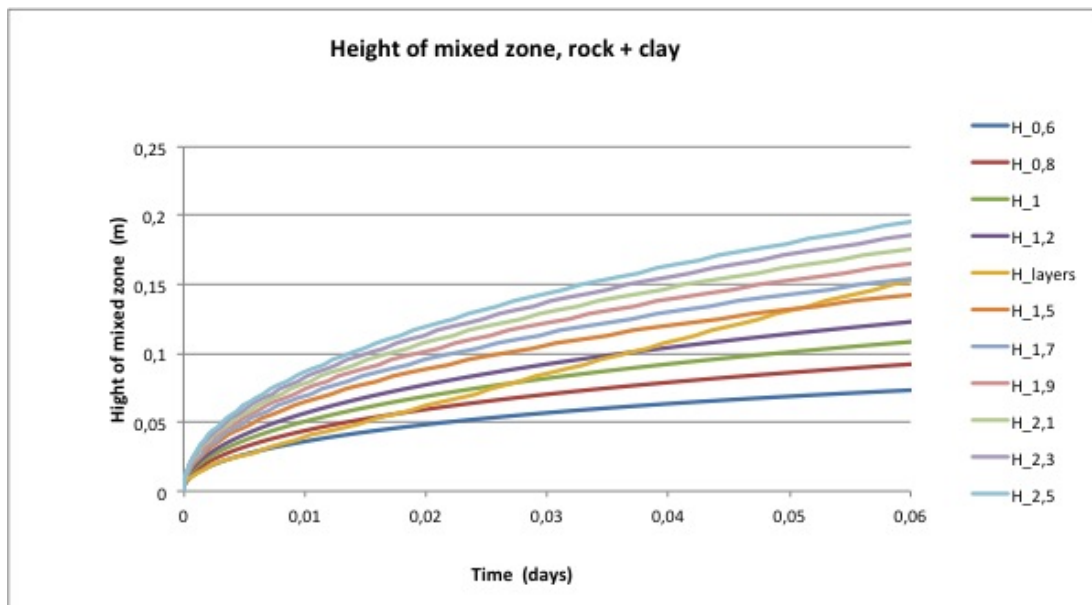


Figure 5.3.1: Example of graph obtained from worksheet

Figure 5.3.1 shows an example of one of the graphs in the worksheet, where all the different levels of the rock fill are taken into consideration, including the condition where the rocks have been laid upon the seabed in layers. The time interval in the graphs is given in days rather than hours or minutes. This is in order to give the experiment some leverage in terms of time perspective, i.e., the experiment can be done over a period of several days or even years if preferred.

## 5.4 Comparing experiments and simulations

The theoretical simulations in the worksheet would ideally be made to fit any condition both rheological and geotechnical in order to only depend on the input parameters in the model. For this to be a possibility, a sort of reference point is needed. And that reference point is what was created by performing experiments on a material similar to that of an offshore clay, and then making the simulations fit accordingly. When comparing the simulations in the worksheet model with the experiments, only experiments 2 and 3 were used, seeing as these showed good results, and better represent the scope of the initial hypothesis. Experiment 1 contains too many uncertainties.

When simulating experiment 2 in the worksheet, a time interval of 6 to 8 minutes between each load step was used, similar to that of the experiment, starting from zero ( $t = 0$ ). The experiments did not start at  $t = 0$  so the graphs had to be modified later in order to get a proper comparison. For each load step in the model an additional height is added to the rock fill, and the corresponding pressure is calculated. The input parameters for the materials (rock, clay, and water), are then introduced.

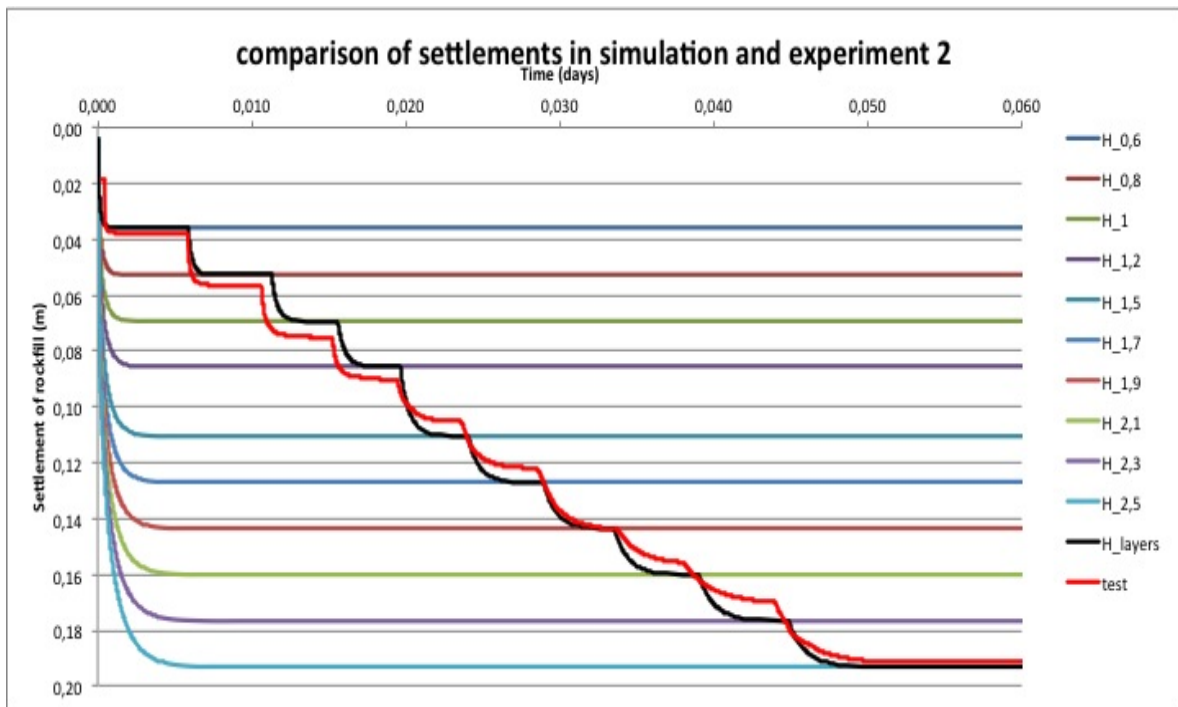


Figure 5.4.1: Comparison of settlements in simulation and experiment 2

The results when comparing experiment 2 and the simulations are shown in figure 5.4.1. The red line in the graph represents experiment 2, and the black line is the corresponding simulation that has been made to fit. As can be seen from the figure the end-value or

final settlement is more or less the same for both the experiment and the simulation, which indicates that the results are good and that the input values make for a decent approximation to the parameters used in the experiment. In order to get the same shape for the simulated line, the viscosity of the clay was the determining factor. Using the measured value from the viscometer as a base,  $\eta = 7,8Pas$ , it was possible to find the best fit to the experimental line. For this experiment the proper viscosity was  $40 Pas$ , giving a permeability of  $39 m/day$ . The lines are not completely matched, but similar curvatures and inclination make for a representative simulation.

For experiment 3 the load steps were changed to intervals of only 5 seconds. This is because the loading had to be done manually, and it was impossible to load  $100kg$  at once, hence there was a 5 second delay for each  $10kg$ . Again using the viscometer result as a reference point for the viscosity, this value is the only change in the input parameters compared to experiment 2. As the viscosity says something about how fast the final settlements are reached we see from this graph that the viscosity has to be lower compared to experiment 2 in order for the lines to fit. The viscosity value that made the best fit was here found to be  $7Pas$ . This value is very similar to the value obtained from the viscometer.

The clay pressure showed a higher maximum value for experiment 3 compared to experiment 2 ( $24,26$  and  $23,59 kPa$  respectively), so the total height of the rock fill was increased slightly.

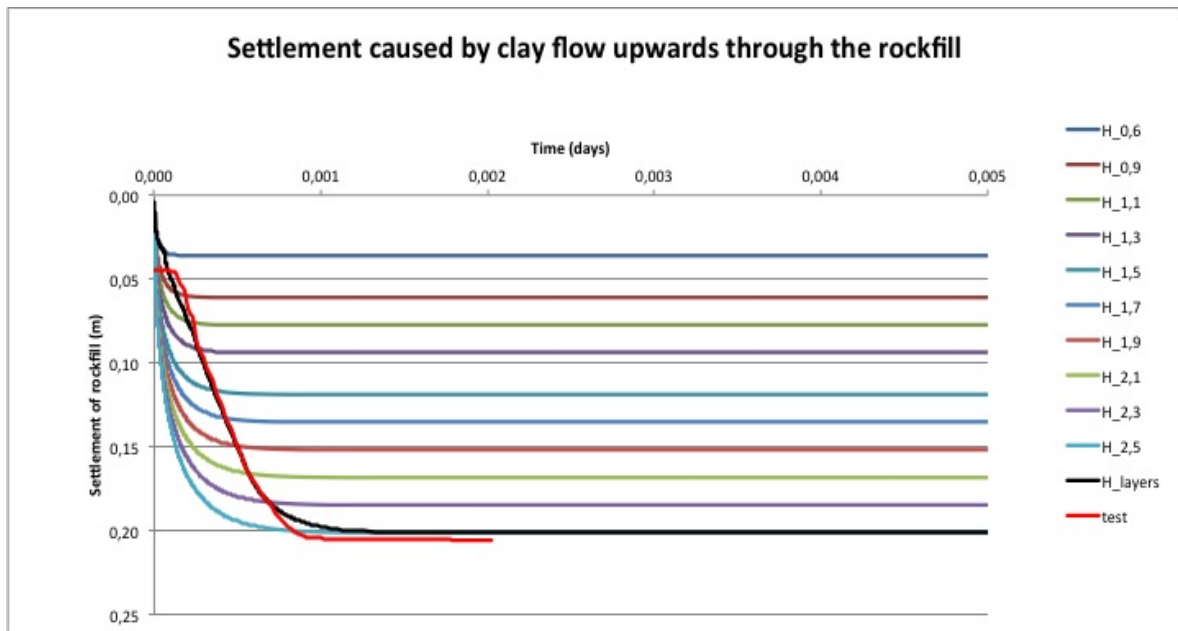


Figure 5.4.2: Comparison of settlements in simulation and experiment 3

Figure 5.4.2 shows that again the final settlements in the simulations are similar in the simulations to those obtained in the experiment.

## Discussion

In general the results were good when comparing the simulation with the experiments. The input parameters for the materials are in the expected range, and therefore the results are realistic. There are some margins for error, however, especially in the rheological formulas. The porosity has been assumed to be 40%, which is the normal porosity value for rock fills when the rocks are dropped at random, but this value was not confirmed in the experiment.

Another aspect is the permeability model. It is assumed here that the Kozeny-Carman model was the best for laminar flow in porous media, but it is not impossible that another model would be more suitable for this specific case. Included in the permeability formula is the surface area. There are several methods for determining the surface area, including the use of different diameters, shape factors, and tortuosity, and here most of these factors are based on scientific assumptions.

The viscometer only provided one singular value for the viscosity, and also in the simulation model only one value for the viscosity is introduced. This is not accurate if the fluid is thixotropic, for which the viscosity decreases with constant shear rate over time. Although the values given work as good estimates. It is also uncertain if the formulas for velocity and settlements in the simulation model are ideal. For experiment 3 the settlements happened so quickly that it is unlikely that the viscosity would have had time to decrease with constant shear rate.

The reason for the different viscosity in experiment 2 and 3 (40 and 7 Pas) respectively, is most likely due to thixotropy. When the time between each load step is longer, the clay will have more time to restructure, and the viscosity will be increase. This makes it harder for the clay to restart at the next load, especially because more rock surface area is covered with each added load, which will increase the frictional forces.

It was evident that for experiment 2 the clay moved in "channels", choosing the easiest path while the remaining clay did not move at all, while for experiment 3 the clay mass moved as a whole through the rocks. More clay probably also formed capillary bonds with the rocks as it passed due to the slow movement in experiment 2, creating suction and reducing the permeability by creating "barriers" of clay. A reduction in permeability creates the same effect as increasing the viscosity. This effect was not as evident in experiment 3 because of the high velocity.

Although there are many probabilities and margins for error, the results from both simulations and experiments support the initial hypothesis and therefore provide a decent indication on the behavior of the interaction between soft clay and rock fill.

## Chapter 6

### Conclusion

The initial hypothesis for this report is that as the rock fill hits the seabed, the soft clay layer will be remolded and act similarly to a fluid, penetrating the rock fill and contribute to increasing the initial settlements. Experiments performed for this report have shown that for sufficiently low shear strengths or sufficiently high water contents in the clay, this theory holds. According to the theoretical simulations the height of the rock fill will determine the magnitude of the final settlements. However, this would not be the case if at a certain shear strength the clay would lose its rheological properties and if the shear strength increases with depth, which could explain why after a given amount of time the settlements are the same for a rock fill of 2 meters as for a rock fill of 0,5 meters. Here the shear strength was the same throughout the material. What finally stopped the rock fill from moving farther in the experiments was the frictional force caused by shearing over the surface area of the rocks and creating a new equilibrium.

The experiments also showed that the time interval at which the loads were applied, or height was added to the rock fill, was a determining factor for the velocity of the clay movement through the rock fill. If 2 meters of rocks are laid upon the seabed at the same time, the total settlements due to clay mixing with the rock skeleton will occur much more rapidly than if the rocks are divided into layers, e.g, 0,5 meters at a time over the course of 1 hour.

The reason for the difference in the velocity of the settlements is partly due to the rheological properties of soft clay. Assuming that clay is a non-newtonian fluid, with the properties of a thixotropic Bingham fluid, the clay will have a yield point in terms of its viscosity. This means that in order for the clay to move at all, the shear stress will have to surpass an initial value. In tests performed in a viscometer this yield value,  $\tau_0$ , was found to be 1,5kPa. This value is higher than expected, but as the method used to determine it was rather uncertain the yield point has been overlooked in the simulations.

The fact that the clay is thixotropic means that the viscosity will decrease with constant shear rate over time, meaning that if the velocity of the movement is kept constant over a long period of time, the viscosity will decrease accordingly. Thixotropy also means that while no shearing is applied to the clay the particles will restructure, and the shear strength will

increase. Due to this the clay moves in "channels", choosing the easiest path in the rock fill. This explains the slow settlements when the rock fill is dropped in layers.

The viscosity of the clay was found in the viscometer to be 7,8Pas. This coincides with the experiment performed with immediate loading where the viscosity was found to be 7Pas through simulations. When the load was applied in layer the experiments and simulations showed a viscosity of 40Pas. This is partly due to thixotropy, and partly due to a limiting of the permeability as more clay "sticks" to the rocks due to suction. The effects of suction will not be as comprehensive with higher velocity because the bonds will not have time to form between the clay and individual rocks.

The hypothesis was only successfully tested for clay with a very low shear strength, 0,35kPa, and it is uncertain whether the effects would be similar for a higher shear strength. An increase in shear strength would not only affect the bearing capacity of the clay, but also the viscosity and the initial yield point would be higher.

More studies on the field are required in order to make a strictly empirically based, working simulation model, but the experiments done here will work as a good base for further work. The interaction or mixing of clay and rocks definitely contributes to the settlements of the rock fill in addition to conventional consolidation theory, and finding a method for reducing these settlements could prevent the loss of thousands of tons of rock in a offshore rock fill.



## Chapter 7

### Recommended future work

Seeing as this whole thesis has been based on trial and error, there is a lot of future work that can be done. The experiments were formed based on discussions on what would be the most realistic approach, and then constructed using whatever could be found in the labs and workshops. And although I am pretty happy with the final setup, there is clearly room for some improvement. More time and planning could shape the experiments into a more realistic procedure.

The most important future work would be to make measurement and do experiments to see the effect of different water contents, or shear strengths, in the clay. In this report, two different shear strengths (0,35 and 0,8 kPa) were studied, and the experiments were only really successful for one of them (0,35kPa). Systematic experiments on different water contents and determination of corresponding viscosities would give a better understanding of the "whole picture". I would suggest measurements of shear strengths in the range of 2 - 0,5 kPa to make sure that all aspects of "liquid-clay" has been covered. Finding the associated viscosities is also very important as the property is assumed to have a big effect on the rate of the settlement. This includes using a more accurate method for finding the viscosity, most preferably a rheometer. A more exact determination and understanding of the thixotropy of the clay would also give a better indication on the effect of time on the material.

Temperature has not been considered here as an effect on the parameters, but could potentially be a huge influence, especially on the viscosity of the clay.

Improving the construction of the equipment used for the experiment would reduce the margin of error. Steel threads shaping the rock fill and barricading the path of the clay should be replaced, preferably with something more elastic. The frame used to stabilize the cylinder caused friction as the cylinder was lowered, nor was it totally stable in all directions. A custom built construction, preferably using the floor as support, would make the experiment run more smoothly.

Further development of the worksheet to include the effect of changing viscosities and increasing shear strength with depth could make the simulations more realistic. More realistic also implies making it more versatile. This could be done by simplifying the setup of the input parameters so that the model could be used in practice without prior knowledge in the field of

rheology. Another aspect of the worksheet that might be improved is the rheological equations. Many of these are largely based on assumptions, and especially the average diameter of the grains in the porous media could be adjusted. For instance finding a way to determine the sauter mean diameter,  $d_{32}$ , would be of great benefit to the accuracy of the surface area of the pores in the rock fill.

In terms of the material used it would be advantageous to use a clay with a lower content of silt particles. This would make the clay more congruent to the material found on the seabed. It would also make the experiments more comparable as silt particles could cause some unwanted friction with the rock fill.

## Appendix A

### Background and task description

# MASTER DEGREE THESIS

## Spring 2012

for

Student: Truls Martens Pedersen

### Initial settlement of rock fills on soft clay

#### BACKGROUND

Rock fills are frequently used as foundations for seabed structures and pipelines. The rock fill consists of crushed rock with grain size 2"-5". The rock fills are usually installed using a fall pipe vessel, and can be constructed with vertical tolerance of +/- 0.2 m at more than 1000 m water depth. An important design criterion for the structures to be placed on the rock fill is the long term settlement.

The long term settlements can be calculated using primary and secondary (creep) consolidation theory. On soft seabed ( $s_u < 2$  kPa) it is however frequently observed settlements not following the consolidation theory. In some cases about 0,3 m settlement has been observed for 0,5 m and 2 m thick rock fills a couple of months after installation. For a settlement process controlled by consolidation and creep a settlement nearly proportional to the fill height is expected.

One possible explanation to the phenomena is that the initial settlement is controlled by a flow of soft clay in to the voids of the rock fill. This process will be governed by the remolded shear strength, the viscosity and thixotropy of the clay (not the permeability and stiffness of the clay).

As long as the physical process controlling the initial settlement is not known, the observed settlements can't be used to calibrate the calculation model for the long term settlement. A better understanding of the initial settlement is therefore important for more accurate prediction of the long term settlement of offshore rock fills

During evaluation of observed settlements of rock fills at the Ormen Lange field, a theoretical model was developed to simulate the flow of clay in the rock fill. This model will be used as a base for the report and modified by performing experiments.

#### TASK DESCRIPTION

The M.Sc thesis should include the following tasks:

- Literature review of the theory primary and secondary consolidation theory and rheological properties for soft clay
- Theoretical study of clay flow in the rock fill void and evaluation of the theoretical background for the proposed model for clay flow.
- Measurement of relevant clay properties (viscosity, thixotropy, shear strength)

- Laboratory test of rock fill penetrating soft clay
- Comparison of laboratory results and the theoretical model

Professor in charge: Gudmund Eiksund

Trondheim, June 06, 2012.



Professor in charge (sign)



## Appendix B

### CD

The CD contains:

- Theoretical model for immediate loading
- Theoretical model for layered loading
- excel file with viscometer data
- Video showing experiment 3 with immediate loading
- The master thesis
- Latex files used in the thesis





## Bibliography

- [1] The concrete portal. webpage, 05 2012.
- [2] Professor A.M.Robertson. Lecture notes on non-newtonian fluids. Part 1: Inelastic Fluids, 2005.
- [3] Knut H. Andersen, Tom Lunne, Tore J. Kvalstad, and Carl F. Forsberg. Deep water geotechnical engineering. Technical report, NGI, 2008.
- [4] Trond Augestad. Viscometer manual. ConTek Viscometer, 05 2012.
- [5] Douglas W. Barr. Coefficient of permeability determined by measurable parameters. *Ground water*, 39(3):356–361, May-June 2001.
- [6] Petter Bryn, Kjell Berg, Carl F. Forsberg, Anders Solheimb, and Tore J. Kvalstad. Explaining the storegga slide. *Marine and Petroleum Geology*, 22:11–19, 2005.
- [7] Pasquale Carotenuto, Carl Fredrik Forsberg, Tom Lunne, and Matt Selvig. Ormen lange 2010 soil investigations. Technical report, NGI, 2010.
- [8] R.P. Chhabra. *Rheology of Complex Fluids*, chapter Non-Newtonian Fluids: An Introduction. Springer Science+Business Media, 2010.
- [9] ConTek. A step forward in concrete technology, 06 2012.
- [10] Guus de Vries; Harald Brennoddén; Joop van der Meer; Stein Wendel. Ormen lange gas field: Immediate settlement of offshore rock supports. *Transactions of the ASME*, 131, 05 2009.
- [11] Dr. S.V. Dinesh. Consolidation of soils. Technical report, Siddaganga Institute of Technology, Tumkur, 2011.
- [12] Leonardo Filippa, Alfredo Trento, and Ana M. Álvarez. Sautermeandiameter determination for the fine fraction of suspended sediments using a lisst-25x diffractometer. *Measurement*, 45(3):364–368, 04 2012.
- [13] Google. Google maps, 04 2012.

- [14] Frantisek Havel. *Creep in soft soils*. PhD thesis, NTNU, 2004.
- [15] The American Heritage. *Science Dictionary*. Houghton Mifflin Company, 2005.
- [16] G.J. Hirasaki. Chap3d. Technical report, Rice University, 03 2004.
- [17] Richard Holdich. *Fundamentals of Particle Technology*, chapter 3. <http://www.midlandit.co.uk>, 2002.
- [18] Thomas Mezger. *The Rheology Handbook*. Curt R. Vincentz Verlag, POB 6247, 30062 Hannover, Germany, 2002.
- [19] Division of Engineering. Porous materials. Technical report, The University of Edinburgh, 2002.
- [20] Truls M. Pedersen. Interview with Gudmund Eiksund, 04 2012.
- [21] Tarald Rørvik. *Geoteknikk: Jordartenes fysiske egenskaper*. Universitetsforlaget, 1 edition, 1971.
- [22] Rolf Sandven. Tba 4110 geotechnics, field and lab investigations. NTNU Geotechnical Division, Trondheim, 2011.
- [23] Josef Sauter. *Die Grössenbestimmung der im Gemischnebel von Verbrennungskraftmaschinen vorhandenen Brennstoffteilchen Die Grössenbestimmung der im Gemischnebel von Verbrennungskraftmaschinen vorhandenen Brennstoffteilchen Die Grössenbestimmung der im Gemischnebel von Verbrennungskraftmaschinen vorhandenen Brennstoffteilchen Die Grössenbestimmung der in Gemischnebeln von Verbrennungskraftmaschinen vorhandenen Brennstoffteilchen*. VDI-Verl, 1926.
- [24] Schlumberger. oilfield glossary, 05 2012.
- [25] Taha Sochi. *Single-Phase Flow of Non-Newtonian Fluids in Porous Media*. PhD thesis, University College Loondon, 07 2009.
- [26] Kansas Geological Survey. Kansas ground water. Technical report, Kansas University, 2005.
- [27] Frank M. White. *Fluid Mechanics*. The McGraw-Hill Companies, University of Rhode Island, sixth edition, 2008.